Mineral Res Expl. Bull., 134, 1-16, 2007

CLAY MINERALIZATION OF THE NEOGENE AGED VOLCANICS OF THE NORTH-EASTERN SİVRİHİSAR (MÜLK-DEMİRCİ)

Zehra KARAKAŞ*, Baki VAROL* and Sonay BOYRAZ*

ABSTRACT.- The Neogene lacustrine units in the Mülk-Demirci region (NE Sivrihisar) are composed of detrital-evaporitic, volcanic and pyroclastic rocks. The Miocene volcanic rocks consist of lava flows of basalt and andesite composition and pyroclastic rocks are made up of agglomerate, tuff, altered tuff and tuffitic sandstone interbedded with altered claystone. These volcanic units change to dolomite, dolomitic limestone, marl and gypsiferous levels to the top. Some alteration zones in tuffs such as iron oxidation, limonitization, carbonatization and argillization are very noticeable with their yellow and red colors. Smectite is the main clay mineral which was formed as a result of alteration of volcanic and pyroclastic rocks in the study area. In some samples, smectite is accompanied mostly by feldspar, dolomite, calcite, opal-CT, quartz and partly by illite, gypsum and analcime. In the electron microscopy (SEM) studies, smectite morphology was distinguished with platy flakes that are developed as a honeycomb texture. In addition, it was also determined in SEM images that smectite mineralization mostly develops in dissolution voids and along fracture and fissures of volcanic glass or on the feldspar minerals. On the basis of field and laboratory studies, formation of smectite was found to be controlled by feldspar and volcanic glass which comprises the main component of tuffaceous units. Under hot and dry climate conditions, alteration of volcanic material in the lake water had an important role in the formation of smectite. Smectite was formed by hydrolysis of volcanic glass and alteration of feldspar.

Key words: Clay mineralization, Neogene, paleoclimate, pyroclastics, smectite, Sivrihisar, volcanic.

INTRODUCTION

The study area is located around the Mülk and Demirci villages (Ankara I27 c4, d3) at 25 km east of Sivrihisar in central Anatolia (Figure 1). Studies in the region were mostly conducted on sepiolite occurrences in the vicinity of study area (Bilgin, 1972; Kulaksız, 1981; Ece and Çoban, 1990; Karakaş, 1992; Gençoğlu et al., 1992; Yeniyol, 1992, 1993; Çoban, 1993; Bellance et al., 1993; Karakaş and Varol, 1993, 1994; Gençoğlu and İrkeç, 1994; Ünlü et al., 1995; Gençoğlu, 1996). The geological characteristics of the basement rocks and Neogene units in the region were studied by Weingart (1954), Erol (1955), Brelie (1956), Umut et al. (1991) and Gözler et al. (1996). Özbaş (2001) investigated mineralogical and geochemical properties of zeolites and associated minerals in the Mülk-Oğlakçı area. Temel (2001) studied geochemistry and petrology of the Miocene alkaline volcanism in the Oğlakçı area.

The aim of present work is to investigate clay mineralization in the Neogene volcanic and pyroclastic rocks around the Mülk-Demirci area and to study the formation conditions of argillization in regard to paleoclimate and bedrock characteristics.

MATERIAL AND METHOD

A total of 35 samples were collected from measured stratigraphic sections of the Karabayırlar Hill I, II, III and Mülk where volcanic, pyroclastic and detrital-evaporitic rocks are widely exposed (Figures 1 and 2). In addition to samples from the measured stratigraphic sections, 30 point samples were also collected from the Çakmak Hill, Çakmakçıkan Hill, Karabayırlar Hill, Hamdere Ridge and Hamam Ridge and around the Asarkale and Mülk villages. Thin sections were made from unaltered rock samples and they were studied with the Leitz brand polarizing microscope to determine their textural and minera-

* Ankara Üniversitesi Mühendislik Fakültesi Jeoloji Müh. Böl. 06100 Beşevler/Ankara
karakas@eng.ankara.edu.tr, varol@eng.ankara.edu.tr, boyraz@eng.ankara.edu.tr

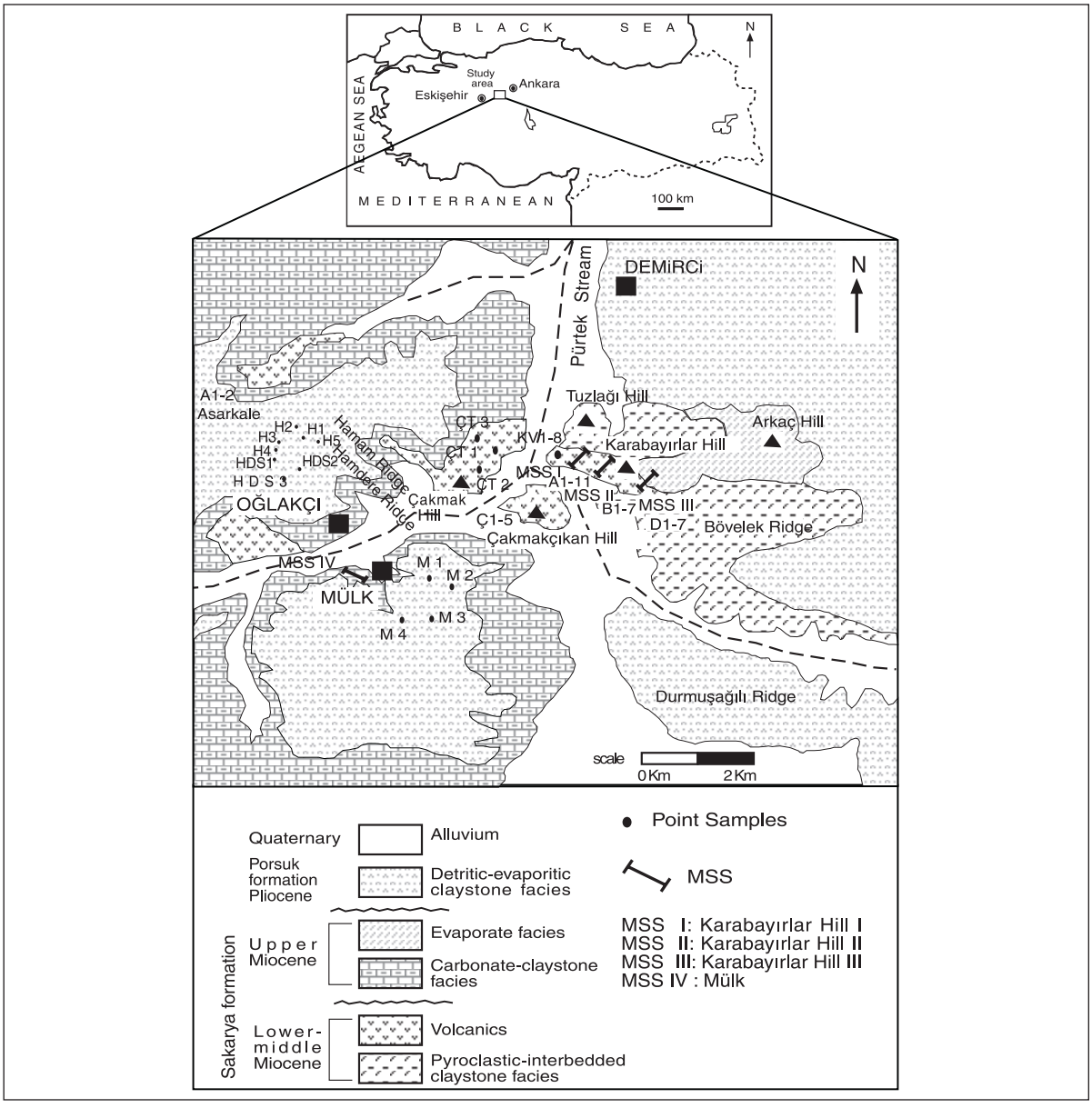

Figure 1- Location and geology map of the study area (Modified from Gözler et al., 1996).

logical properties. Volcanic and pyroclastic rocks were classified according to Streckeisen (1976, 1979) and Schimid (1981), respectively. Mineralogical compositions of clay minerals and partly and completely altered rock samples were determined with Rigaku-Geirgeflex X-Ray Diffractometer (XRD) device with whole rock (45 samples) and clay fraction (35 samples) analyses. Semi-quantitative mineralogical analysis of the samples was done (Gündoğdu, 1982) by the external standart method (Brindley, 1980). The morphologic properties and textural characteristics of samples which are dominated by argillization were studied with JEOL 840 A brand scan-

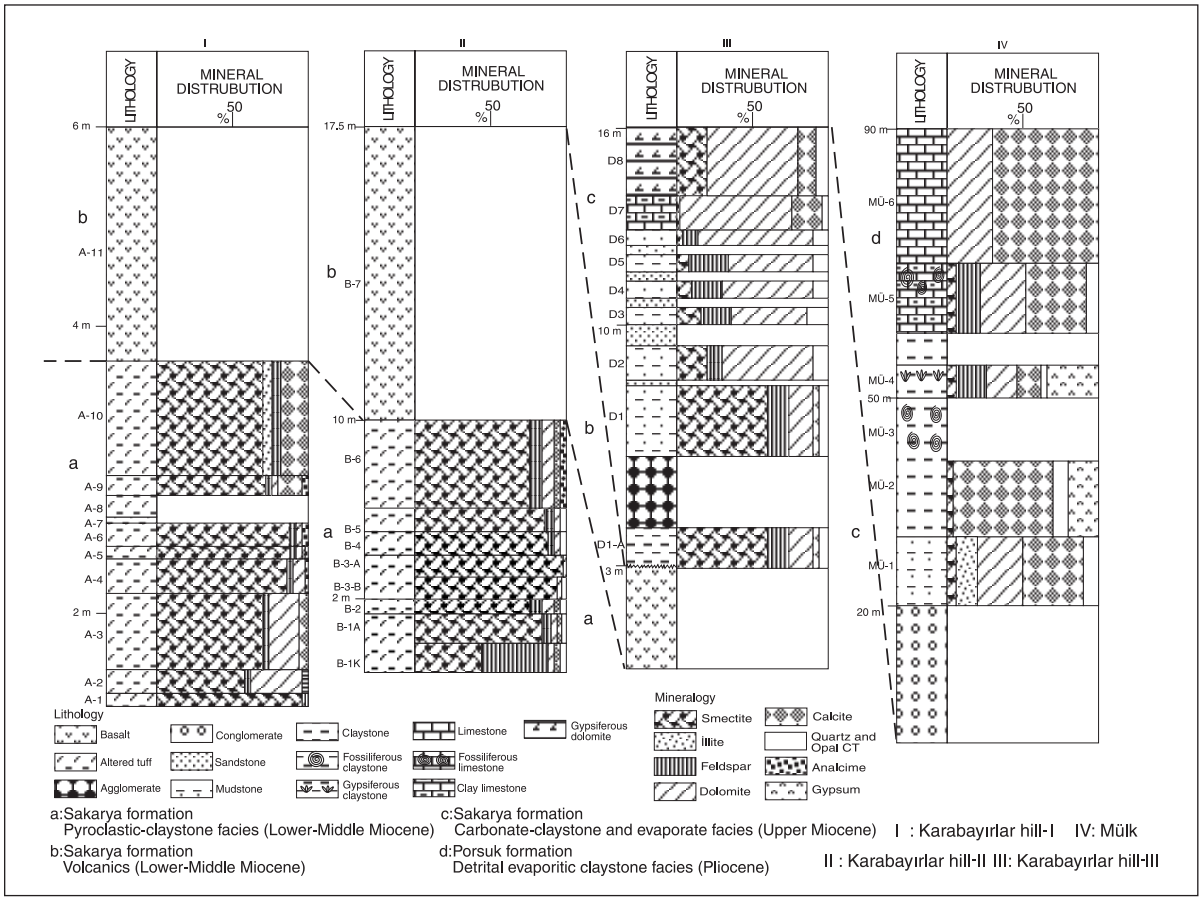

Figure 2- Lithological and mineralogical distribution in the Sakarya and Porsuk formations in the study area.

ning electron microscope (SEM). Moreover, thermal behaviors of clay minerals were determined with Rigaku Analyzer TAS 100 device at the General Directorate of Mineral Research and Exploration of Turkey (MTA).

GEOLOGY

The basement of the Sivrihisar Neogene basin is represented by Paleozoic metamorphic rocks consisting of schist, gneiss and marble and Mesozoic ophiolitic complex, granite and granodiorites (Kibar et al., 1992; Gözler et al., 1996). Exposures of the basement rocks are observed around the Sazak and Baharözü villages at NE of Sivrihisar town, outside of the study area. The Neogene units which have a wide distribution in the region unconformably overlie the basement rocks. In previous geologic and industrial raw material studies conducted in and around the study area, Neogene units were investigated under different formation names. Gençoğlu and İrkeç (1994) described the lacustrine units as the İlyaspaşa (Miocene) and Sakarya (Pliocene) formations while the same units were named as the Porsuk (Miocene) and Hüyüklü (Pliocene) formations by Gözler et al. (1996). In the present work, lacustrine units in the area were described as Miocene Sakarya and Pliocene Porsuk formations (Boyraz, 2004) (Figures 1 and 2). The mappable lithofacies of the Sakarya formation, from bottom to the top, are pyroclastic - interbedded claystone, volcanics, carbonate - claystone and evaporate facies. The pyroclastic - interbedded

claystone facies is represented by agglomerate, tuff, altered tuff and tuffitic sandstone. Altered claystone levels and tuff levels which are mostly observed in multi-colorings are repeatedly alternated (Figure 3a, b). In addition to argillization, iron oxidation, limonitization and carbonatization are also detected in tuffs (Figure 3c). These alteration zones are noticeable with yellow, red, greenish yellow and green colors. Volcanics overlying the pyroclastic-interbedded claystone facies are observed as basaltic and andesitic lava flows (Figures 1, 2 and 3a). Basalts show porphyry-afanitic texture and gas vesicles while andesites are characteristic with light pink-beige colors, compact structure and afanitic texture. Basalts and andesites that are observed as partly or completely altered are typical with yellow, red and reddish brown colors. The volcanics in the region are exposed along E-W extending fault systems which were developed as a result of N-S extending compressional regime which was followed by an extensional tectonism (Temel, 2001; Özen and Sarıfakıoğlu, 2003). Basalts and andesites in the study area were dated as Early-Middle Miocene (14-18 Ma) (Temel, 2001). These volcanics are overlain with a low-angle angular unconformity by carbonate-claystone and evaporate facies which is represented from bottom to the top by dolomite, dolomitic limestone, mudstone and gypsiferous units (Figures 1, 2 and 4). Some Gastropod species such as *Planorbarius* sp., *Lymnaea* sp., *Helix mrazeci* Sévastos, 1922, *Abida* sp. and *Mostus* sp. (Upper Miocene) were determined in clay, marl and organic material-rich units in this facies (Taner, 2004). On the basis of data obtained from radiometric and paleontological dating studies, the age of the Sakarya formation is accepted as Miocene.

The Sakarya formation is overlain with a low-angle angular unconformity by detritic-evaporitic claystone facies of the Pliocene Porsuk formation (Figures 1). This facies is composed of a repetition of deposition package consisting of red-gray colored conglomerate-sandstone, gray-green colored claystone, gypsum, gypsiferous mudstone, dolomite, dolomitic claystone and limestone (Figures 1 and 2). Some Gastropod species such as *Valvata crusitensis* (Fontannés, 1886), *Gyraulus* (G.) *ignoratus* Schickum-Puissegur, 1977, *Emmericia rumana* Tournouér, 1880 were determined in green claystone and marl units and the age of the Porsuk formation is accepted as Late Pliocene (Romanian) (Taner, 2004). In addition, in these units, some ostracoda fossils such as *Ilyocypris* sp, *Potamocypris similes* (Müller, 1894), *Pseudocandona* cf. *compressa* (Koch, 1837), *Hemicyprideis dacica grekoffi* Carbonnel, 1971, *Cyprideis* cf. *torosa* (Jones, 1850), *Candona neglecta* Sars, 1888, *Candona* sp. were also found which yielded Pliocene-Early Pleistocene age. Moreover, spore-pollen studies conducted on brown clayey, clay, marl and organic material-rich units yielded the presence of biozone assemblages which indicate Late Pliocene age. These assemblages are Tubuliflorae and Liguliflorae types (Batı, 2004). In addition, this dating was also verified by micro/macro mammalian assemblages such as *Testudo* sp., *Micromys* sp., *Occitamomys* sp., *Prolagus* sp. and *Promimomys* sp. (Saraç, 2004).

Red colored Quaternary units which unconformably set above the Neogene lacustrine deposits are composed of red-brown conglomerate, mudstone, sandstone and alluvium.

PETROGRAPHY

Regarding mineralogical compositions and textural characteristics, volcanic and pyroclastic rocks in the study area were described as tuff, basalt and andesite.

On the basis of their rock fragment, volcanic glass and crystal content abundance, tuffs comprising the dominant lithological assemblage of pyroclastic rocks are investigated as lithic, vitric and crystal tuff. The vitric tuffs are completely composed of volcanic glass. In volcanic glass which is generally observed as fragmented and rounded grains, some alteration products such

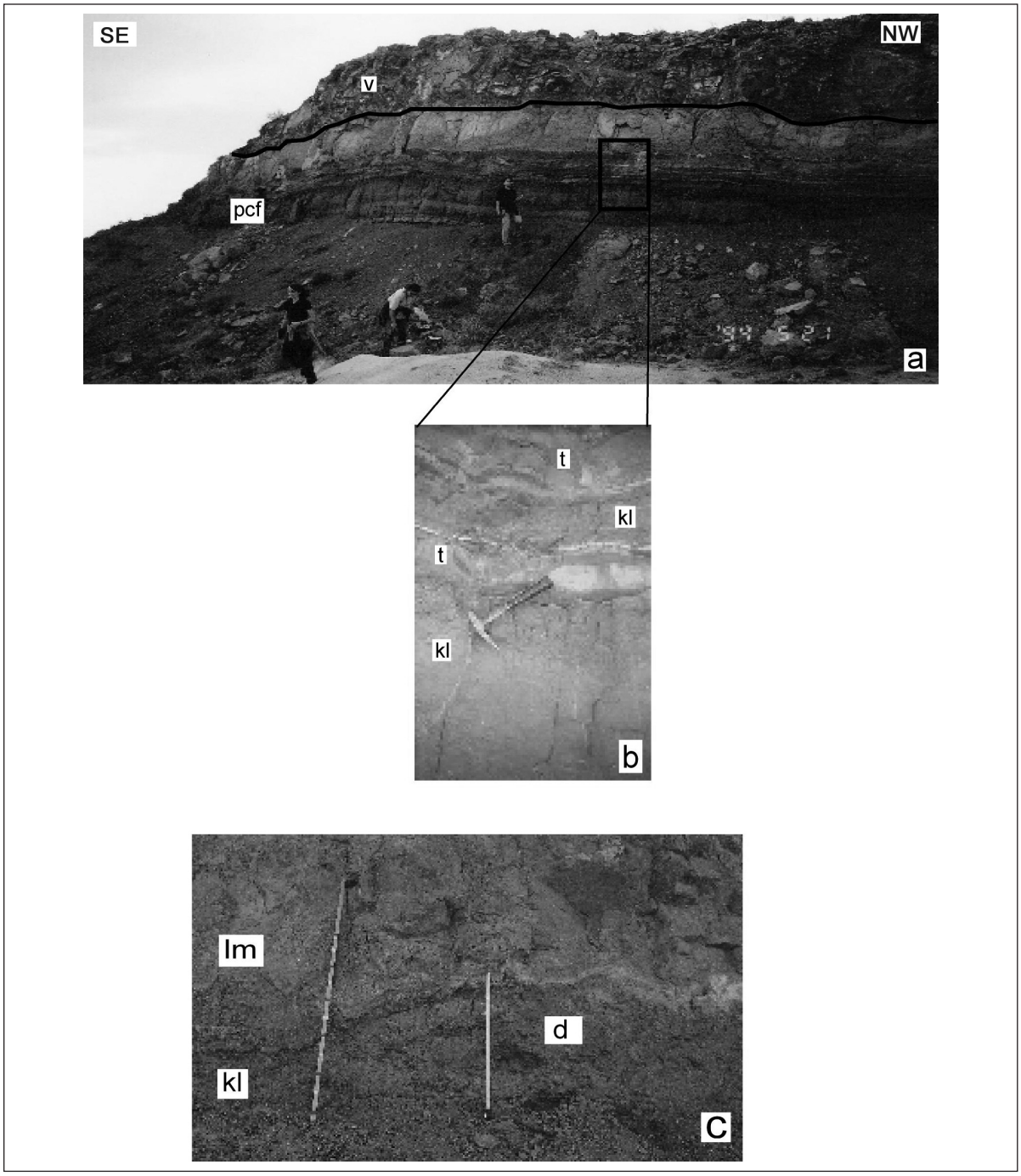

Figure 3- a. Vertical and horizontal relations between pyroclastic-interbedded claystone facies (pcf) and volcanics (v) at the Karabayırlar Hill;
b. Close view of multicolored, altered tuffs (t) and alternated claystone levels (kl);
c. Argillization (kl), limonitization (lm) and iron oxidations (d) in the pyroclastic-interbedded claystone facies.

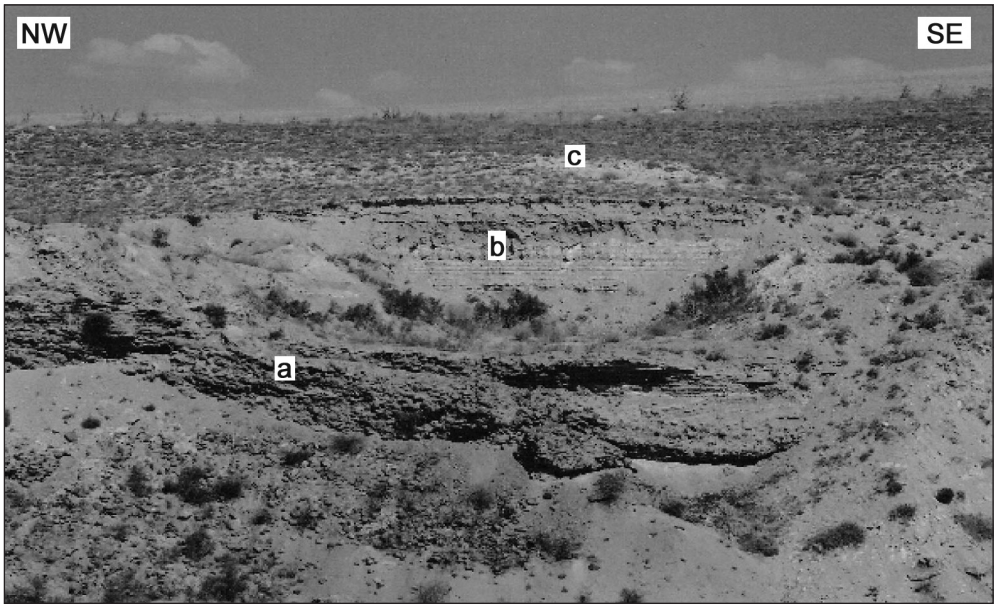

Figure 4- The transition between pyroclastic-interbedded claystone facies (a), carbonate-clay stone (b) and evaporate (c) facies.

as argillization and carbonatization are partly noticeable (Figure 5a). Lesser amount of opaque mineral was also determined in the volcanic glass. In the study area, vitric tuff was intensely found at the Karabayırlar Hill (MSS I and II) (Figures 1, 2). The lithic tuffs are made up dominantly of volcanic rock fragments (andesite) and partly of quartz and biotite phenocrystals (Figure 5b). Litic tuffs were also observed at the Karabayırlar Hill (MSS I and II) (Figures 1, 2). The crystal tuffs are composed of plagioclase, biotite, hornblende and quartz phenocrystals and volcanic glass. The flow texture observed in crystal tuffs is noticeable with oriented plagioclase microcrystals and biotite and hornblende are partly or completely transformed to opaque minerals (Figure 5c). Like vitric and lithic tuffs, the crystal tuffs are also observed at the Karabayırlar Hill (MSS I and II) (Figures 1, 2).

The basalts in the area have porphyric hypocrystalline texture. In addition, amigdaloidal texture is also observed which is formed by filling of gas vesicles with the secondary quartz crystals. The rock is composed mainly of plagioclase and pyroxene phenocrystals together with microlite and crystallites (Figure 5d). Labrador plagioclase displays alteration signs such as iron oxidation, carbonatization and argillization. Most part of pyroxene phenocrystals were iddingsitized and form glomeroporphyric texture. In the study area, basalts are exposed at the Karabayırlar (MSS I and II), Çakmak and Çakmakçıkan Hills (Figures 1, 2).

Andesites are composed of plagioclase (andesine), hornblende and biotite and show trachytic texture. Plagioclases are subhedral and display a zoning texture (Figure 5e). In addition, hornblende and biotite are transformed to opaque form (Figure 5f). Their typical exposures are found around the Asarkale (Figure 1).

XRD DETERMINATIONS

In order to determine the relation between bedrock and clay minerals which were formed in association with alteration of volcanic and pyro-

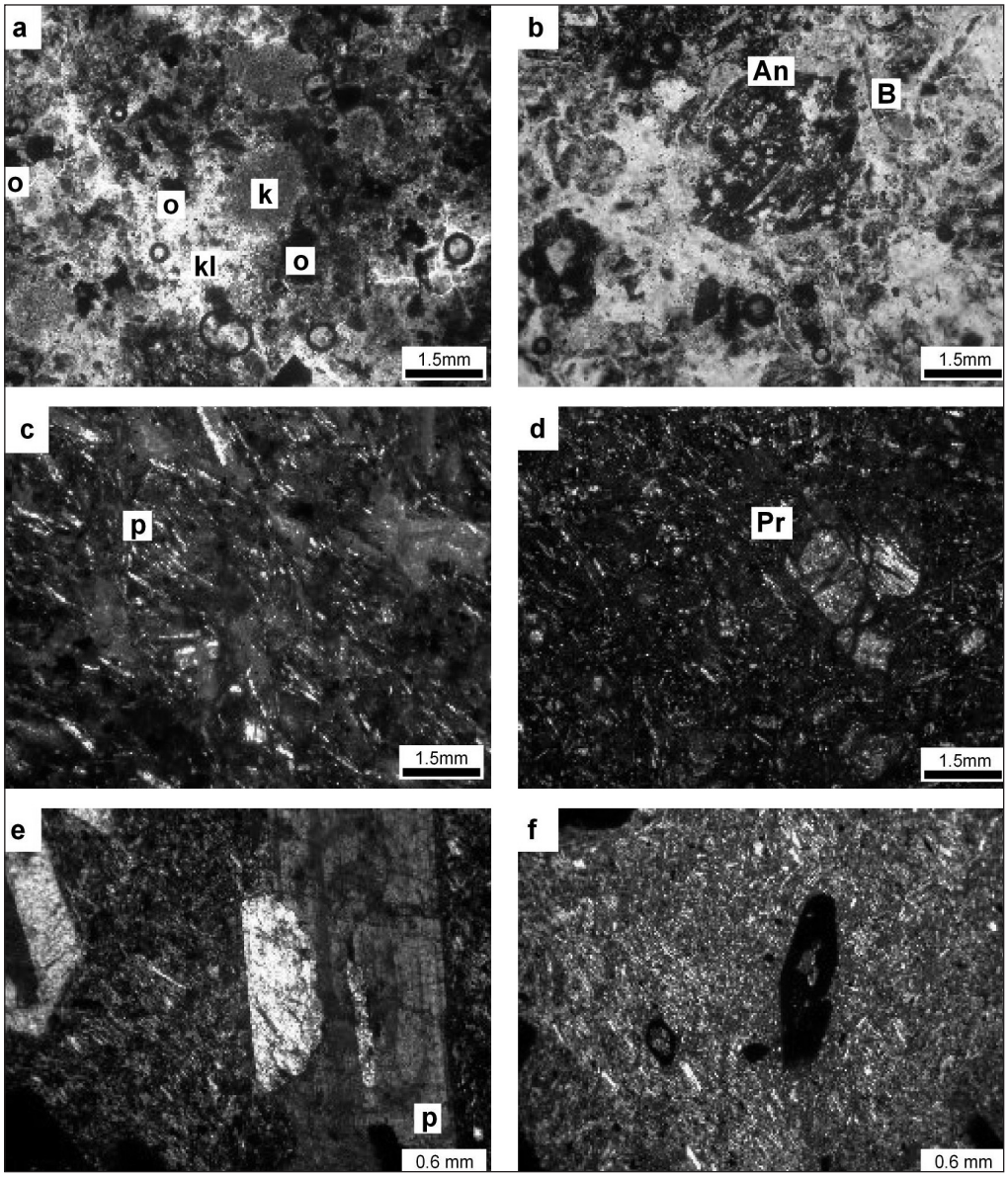

Figure 5- Microscopic views of pyroclastic and volcanic rocks:

a- Argillization (kl) and carbonatization (k) developing in volcanic glass of vitric tuffs and opaque minerals (o) (under crossed polars - sample no. A-4);

b- Andesite (An) rock fragment and biotite (B) phenocrystal in lithic tuffs (under plane polarized light, sample no. A-5);

c- Plagioclase (p) microlites oriented with flow texture observed in crystal tuffs (under crossed polars - sample no. A-9);

d- Pyroxene (pr) phenocrystals and plagioclase microlites which display iddingsitiza tion along edges and fissures of basalts (under crossed polars - sample no. Ç-2);

e- Sub-hedral and zoning plagioclase (p) phenocrystals in andesites (under crossed polars - sample no. A-1);

f- Opaqued hornblende in andesites (under crossed polars - sample no. A-2).

clastic rocks, fresh and altered samples from these units were analyzed with XRD method.

Clay fraction studies of volcanic and pyroclastic units indicate that the dominant clay is smectite although illite exists in a few samples (Figures 2 and 6a). The abundance of smectite varies with the alteration degree of volcanic and pyroclastic rocks. In intensely altered samples, smectite is the main clay mineral (90%-100%) (Figures 2 and 6a). In moderately less altered samples, the abundance of smectite in whole rock analysis was found to be ranging from 40 to 70% (Figures 2 and 6b, c). In whole rock analysis, smectite is accompanied by feldspar, dolomite, calcite, opal-CT, quartz and lesser amount of illite, analcime and gypsum (Figures 2 and 6a, b, c). In the analysis, smectite was described with the maximum peak intensity at 15.12 A° - 15.93 A° which belongs to (001) reflection surface (Figure 6a, b, c). In addition, peaks at 5.06 A°, 4.49 A° and 2.56 A° with higher 2 values were also helpful for identification of smectite. The intensity of (001) peak which is the first basal reflection is narrow and symmetrical thus indicating that smectite is well crystallized. According to 14.76 A° -15.93 A° (001) reflection values, smectite was determined as Ca type smectite (Moore and Reynolds, 1989) (Figures 6a, b, c).

In whole rock analysis, feldspar was identified at 3.18 A° - 3.20 A° and 3.22 A°, dolomite at 2.89 A°, calcite at 3.04 A°, quartz at 3.34 A° and analcime at 3.43 A° peaks (Figures 6a, b, c). In whole rock analysis of samples which were altered at varying degrees and contain smectite as the only clay-size component, there exists a proportional inverse relation between smectite and feldspar (Figure 2). In samples which are particularly intensely altered and enriched in smectite, the feldspar content decreases while in samples which are less altered and represented by low smectite content, the feldspar content shows a proportional increase (Figures 2 and 6a, b, c).

(001) reflection of smectite which was treated with ethylene glycol shifted to 16.67 A° (Figure 7). The reflections at 350 and 550ºC were observed at 9.66 A° and 9.76 A°, respectively.

In X-ray diffractograms of whole rock samples, rising of background by 2θ = 15 A° indicates the presence of volcanic glass of amorphous character (Jones and Segnit, 1971).

DTA DETERMINATIONS

Thermal characteristics (phase transformations) of sample B3A which was determined as smectite by XRD studies were studied with DTA-TG analysis. In DTA analysis of smectite, the first intense endothermic peak was observed around 148.2 °C (Figure 8). The second small endothermic peak at 220 °C is typical for Ca-smectite (Özkan and Erkalfa, 1977). In addition, there are also two endothermic peaks at 653.4 °C and 873.1 °C. Temperatures of these endothermic peaks are suitable for dioctaedric smectites (Paterson and Swaffield, 1987). The first two endothermic peaks reflect the humidity loss and the third one stands for the loss of interlayer water. The weight loss in the first two reactions is 15.3% and 7.6% in the third reaction (Figure 8). The peak observed at 810.1 °C at the DTA curve is related to impurities rather than smectite.

SEM DETERMINATIONS

The clay-dominant (smectitization) samples which were by determined to be variously altered by field observations, microscopic investigations and XRD analyses were also studied with scanning electron microscope (SEM).

In scanning electron microscope studies, it was observed that smectite has a well developed platy structure and morphology of honeycomb texture (Figure 9a). In general, smectite develops in fissures, fractures and dissolution voids of the volcanic glass (Figure 9b). It was noticed that the smectite with honeycomb texture develops on spherical opal-CT (Figure 9c). In some samples, smectite develops on and along the edges of feldspar as well as volcanic glass (Figure 9d).

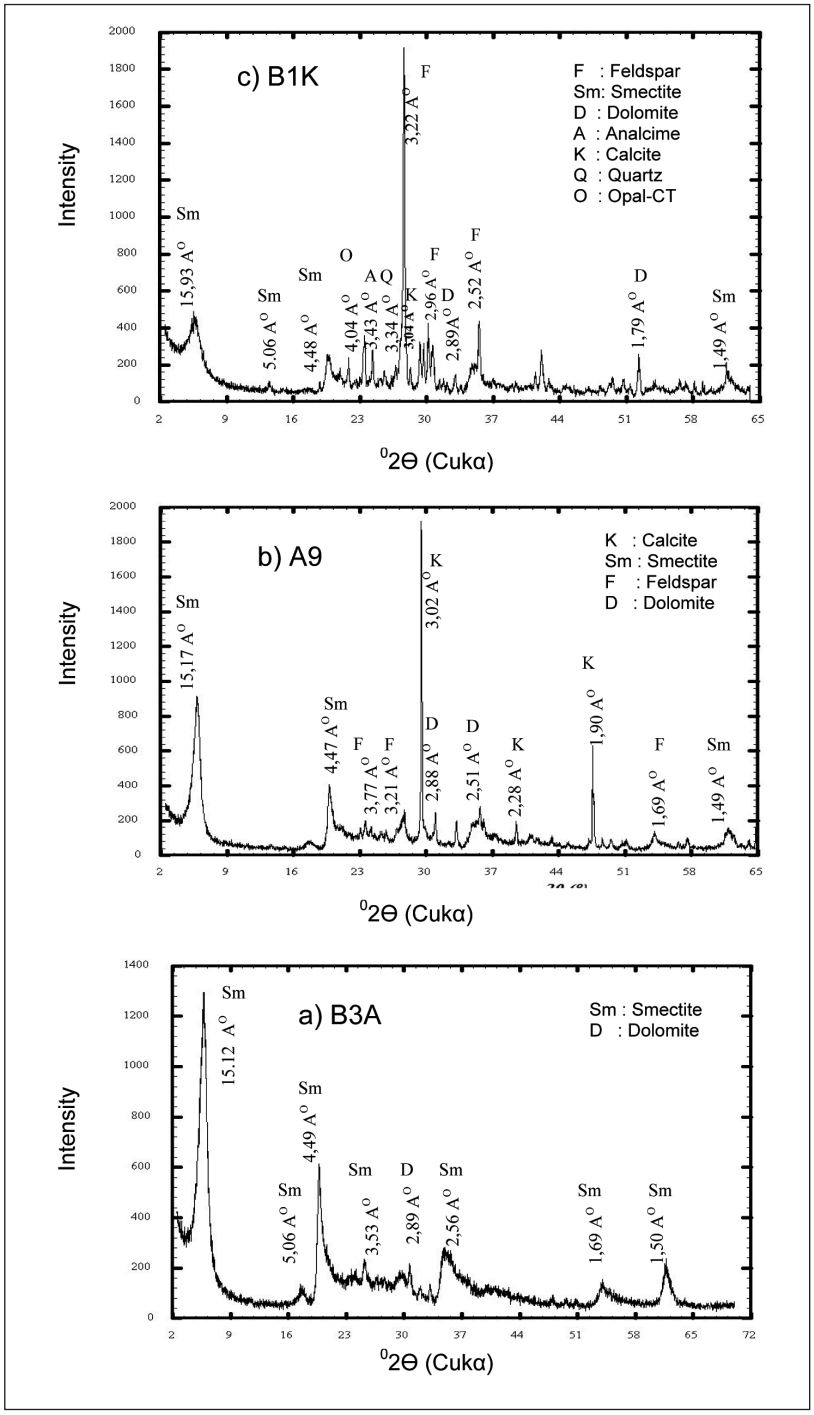

Figure 6- Whole rock XRD diffractogram of tuff samples which were altered in varying degrees (a. altered tuff, sample no. B3A; b. less altered tuff sample no. A9; c. partly altered tuff, sample no. B1k).

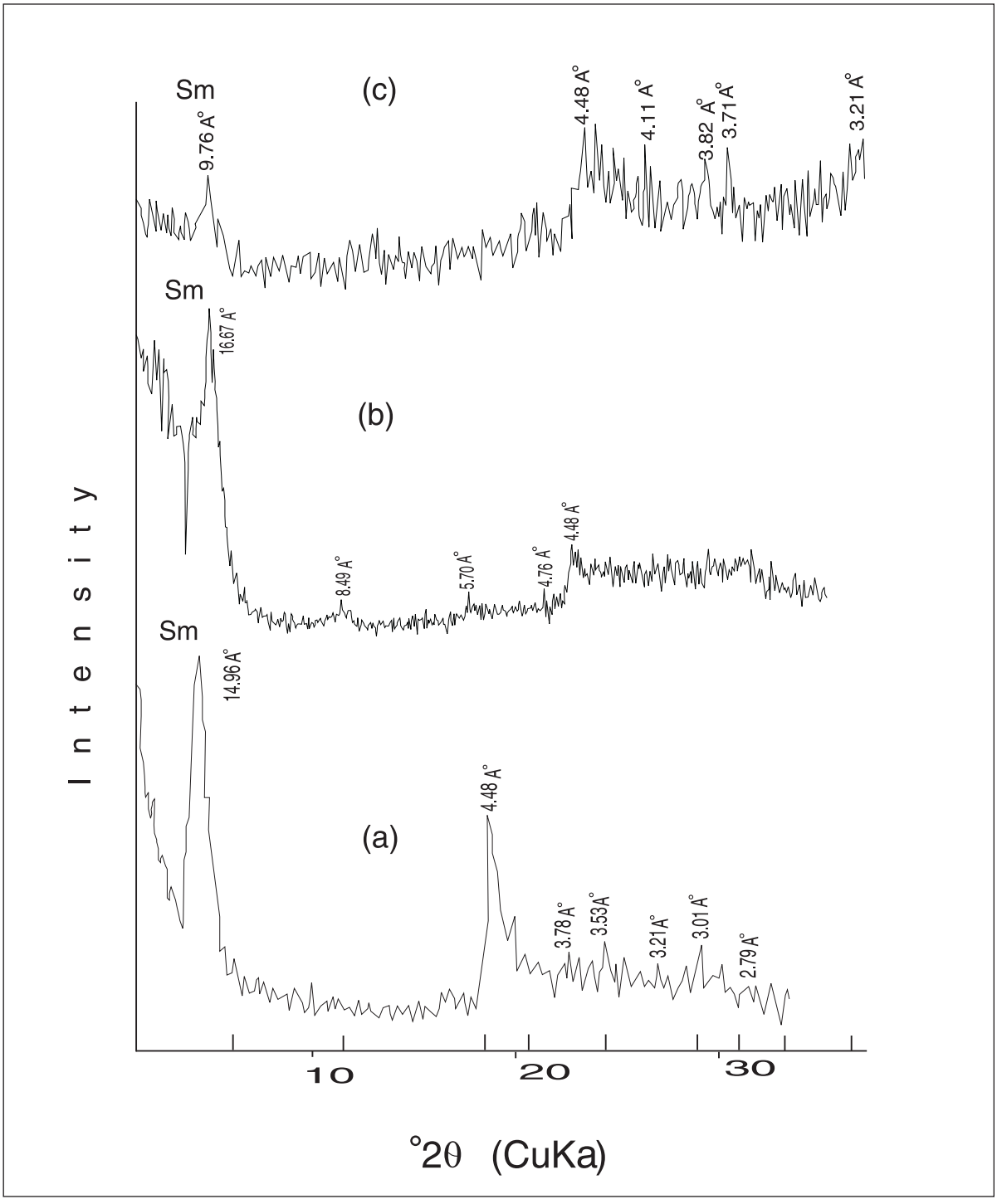

Figure 7- XRD diffractogram of clay fraction of nearly pure smectite (sample no B3A), a: normal; b: glycolated; c: heated (550ºC).

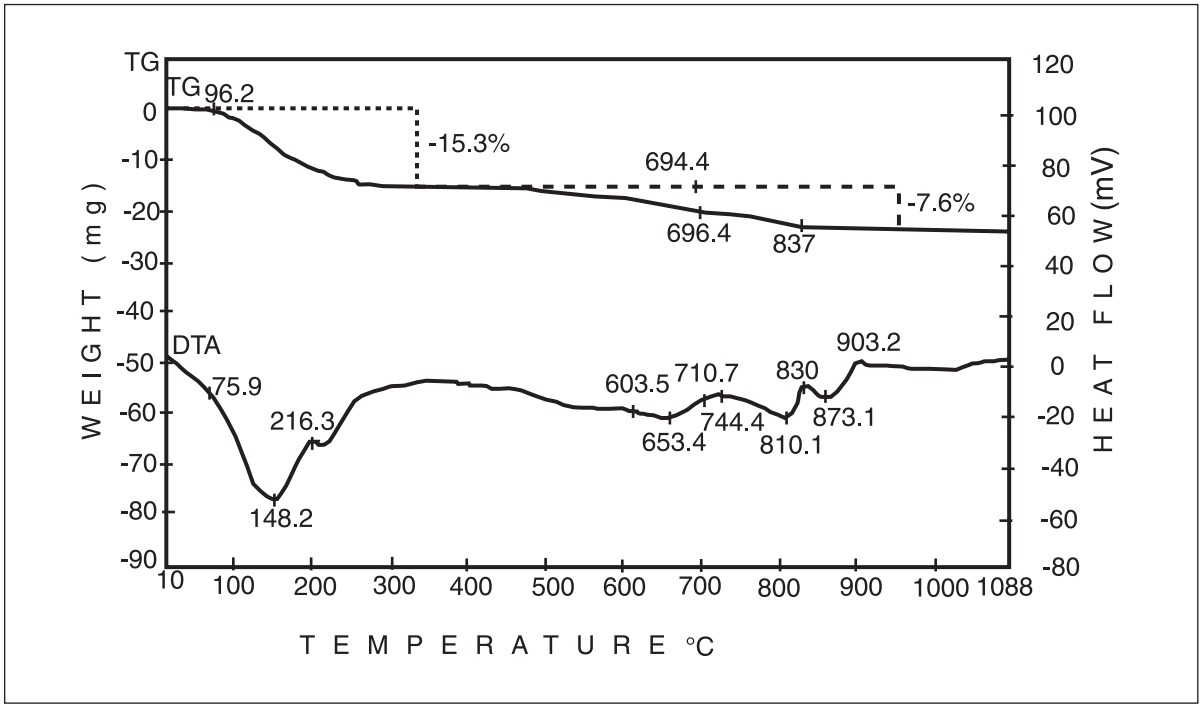

Figure 8- DTA and TG thermogram of nearly pure smectite (sample no B3A).

This may indicate that in addition to volcanic glass and opal-CT, feldspar also had a role in formation of smectite. Christidis et al. (1995), Kadir and Karakaş (2002), Besbelli and Varol (2002) also indicated that smectite was derived from alteration of volcanic glass and feldspar.

DISCUSSION AND RESULTS

The Neogene lacustrine units which are widely exposed in the study area are described as the Miocene Sakarya formation and Pliocene Porsuk formation (Figures 1 and 2). The Sakarya formation starts with pyroclastic-interbedded claystone facies that is characterized by agglomerate, tuff, altered tuff and tuffitic sandstone and continues with a volcanic sequence (Lower-Middle Miocene) represented by lava flows of basalt and trachyandesite composition. These units are overlain with a low-angle angular unconformity by carbonate-claystone and evaporate facies (Upper Miocene) which are composed of claystone, dolomite, limestone, mudstone and gypsum. The Pliocene units which cover this lithologic assemblage with a low-angle angular unconformity are comprised by a repetition of sequence consisting of conglomerate, sandstone, claystone, mudstone, gypsum, gypsiferous mudstone, dolomitic claystone and limestone.

According to field and laboratory observations, Neogene (Miocene and Pliocene) lacustrine units in the region were deposited under varying volcanism, tectonism and paleoclimate conditions. In this respect, there are different facies in the study area showing horizontal and vertical changes. The volcanic activity in the region was started in the Early-Middle Miocene (Temel, 2001; Özen and Sarıfakıoğlu, 2003). In the first period of deposition when the volcanism was active, lacustrine deposits which were originally depleted in evaporitic minerals were changed to dolomite-evaporite facies with increasing evaporation at arid and sub-arid climate conditions.

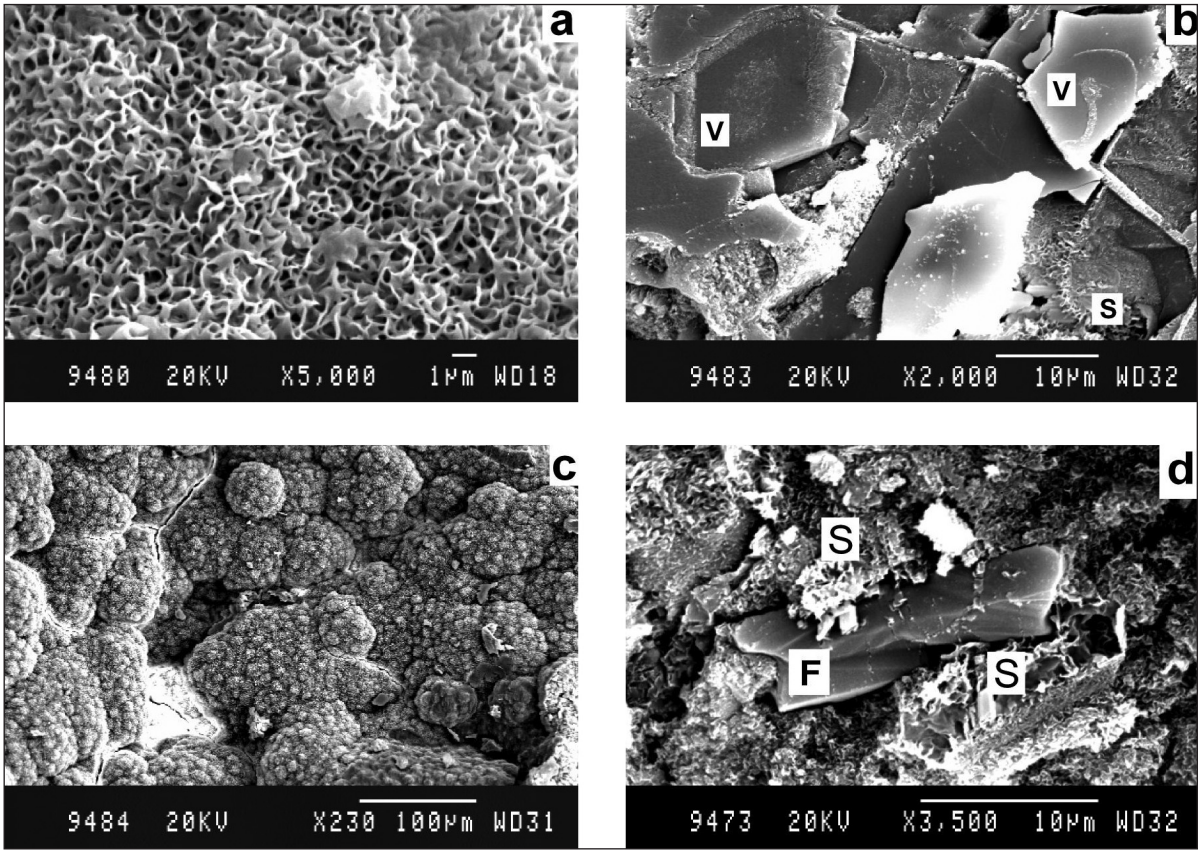

Figure 9- SEM image of smectites.
a: Platy and honeycomb textured smectite (sample no B-1);
b: Smectite mineral developing along edges and surfaces of fractured, platy volcanic glass (V) (sample no KV-8);
c: Smectite forming on spherical opal-CT (sample no KV-8);
d: Smectite (S) developing around and on the feldspar mineral (F) (sample no B-5).

It was determined that smectite is the main clay mineral in alteration zones of tuff and basalts which comprise the volcanic and pyroclastic units of the Sakarya formation. Considering the role of whole rock assemblage and textural characteristics in formation of smectite, alteration of volcanic ash and tuff is the main agent for the deposition of smectite (Grim and Güven, 1978). Particularly, smectite formation was controlled by the presence of volcanic glass and feldspar which are the main components of tuffaceous units. In XRD studies, in addition to the association of volcanic glass, opal-CT, smectite and feldspar which comprise the main components of volcanic units, a proportional inverse relation between smectite and feldspar was also determined which indicates that these minerals are derived from the same source (Figures 2, 6 and 9). Alteration of feldspars results in formation of smectites (Millot, 1970; Furnes, 1975; Chamley, 1989; Tucker, 1992; Kadir and Karakaş, 2002). Alteration of feldspar facilitated great amount of Ca input to the environment which is supported by carbonates occurrences partly shown in fractures. In addition, gypsum was precipitated with the increase of Ca and SO_4 activities due to arid conditions of the environment (Yeniyol, 1987).

Under hot and arid conditions, alteration of volcanic material in the lake water had an important role in formation of smectite. This is in support of the presence of dolomite above the volcanic units which reflects hot and arid climate regime in the area. Smectite is related to hot-arid climate regime and it is known to occur under low rainfall and weak drainage conditions (Chamley, 1989). In addition, it is stated that analcime which is accompanied with smectite in some samples, is occured in saline and alkaline lacustrine environment, indicating that arid and semi-arid climate conditions (Mariner and Surdam, 1970; Gall and Hyde, 1989; Hartley et al., 1991; Renaut, 1993; Türkmenoğlu et al., 1995; Karakaş and Kadir, 2006). While arid conditions were prevailing in the region, units were deposited in association with depth changes in the lake which rapidly deepened due to increasing tectonic activity. The change in lithology in the environment depending on change of depth in the lake area was studied by Hardie et al. (1978). Waters which affected the porous and permeable volcanic units in the study area washed and dissolved the tuffaceous units. Smectite was formed as a result of hydrolysis of volcanic glass and alteration of feldspar. As also evidenced in SEM studies, smectite occurs in weak zones developing in dissolution voids and along the fissure and fractures of volcanic glass indicating that ions freed by water circulation were effective in formation of smectite. Stages which follow the forming of smectite, contributes to rich in Na, Al, and K ions of lacustrine water and increasing pH, resulting in analcime occurrences (Gall and Hyde, 1989; Stamatakis, 1989; Hartley et al., 1991, Karakaş and Kadir, 2006). Illite minerals accompanied with smectite in altered tuff samples were derived from clay-sized biotite (Bayhan and Yalçın, 1990; Gümüşer and Yalçın, 1998). On the contrary, illite minerals in mudstone samples were originated from detritic form and was transported to lacustrine environment.

As a result, formation of smectite was controlled by the presence of volcanic glass and feldspar that comprise the main components of volcanic and pyroclastic rocks. Alteration of volcanic material in the lake water under hot and arid conditions had an important role in the smectite formation. Formation of smectite is closely related to hydrolysis of volcanic glass and alteration of feldspar.

ACKNOWLEDGEMENTS

This study was supported by the Scientific and Technical Research Council of Turkey (TUBITAK Project No. 102Y137) and the Ankara University under grant No. 2003-07-45-014. This work is a part of third author's master thesis. Authors are grateful to Prof. Güler Taner (AU) for her contribution to paleontologic studies, Zühtü Batı (TPAO) for performing the pollen analyses and Dr. Gerçek Saraç (MTA) for the mammalian determinations, Prof. Dr. Asuman Türkmenoğlu (METU) and Prof. Dr. Emel Bayhan (HU) for their constructive critical comments and suggestions on the manuscript.

Manuscript received on July 12, 2006

REFERENCES

Batı, Z. 2004. Sözlü Görüşme. Türkiye Petrolleri Anonim Ortaklığı.

Bayhan, E. and Yalçın, H. 1990, Burdur gölü çevresindeki Üst Kretase - Tersiyer yaşlı sedimanter istifin tüm kayaç ve kil mineralojisi. Maden Tetkik ve Arama Dergisi, 117, 73- 87.

Bellanca, A., Karakaş, Z., Neri, R. and Varol, B. 1993. Sedimentology and isotope geochemistry of lacustrine dolomite-evaporite deposits and associated clays (Neogene, Turkey): environ mental implication. Mineralogica et Petrographica Acta, 36, 245-264.

Besbelli, A. and Varol, B. 2002. Tekke volkanitlerinde hidrotermal alterasyon ürünü kil mineralleşmeleri (Çubuk, Ankara KD). Maden Tetkik ve Arama Dergisi, 125, 121 -137.

Bilgin, H. 1972. Eskişehir ili kil imkanlarının genel ekonomik prospeksiyon raporu. Maden Tetkik Arama Genel Müdürlüğü Rapor No: 4708, 38s. Ankara (unpublished).

Boyraz, S. 2004. Mülk-Demirci yöresi (Eskişehir-Sivrihisar) Neojen (Üst Miyosen-Pliyosen) birimlerinin kil mineralojisi. Ankara Üniversitesi Fen Bilimleri Enstitüsü Yüksek Lisans Tezi, 85s, Ankara (unpublished).

Brelie, V.G. 1956. Sivrihisar ve Polatlı bölgesinde yapılan bir linyit prospeksiyonu hakkında rapor. Maden Tetkik Arama Genel Müdürlüğü Rapor No: 2437, Ankara (unpublished).

Brindley, G. W. 1980. Quantitative X-Ray Mineral Analysis of Clays. In: Brindley, G W. and Brown, G (ed). Crystal Structures of Clay Minerals and Their X-Ray İdentification. Monograph 5, Mineralogical Society, London, 411-438.

Chamley, H. 1989. Clay formation through weathering. In: Chamley, H. (ed.). Clay Sedimentology, Springer Verlag, New York, 21-50.

Christidis, G.E., Scott, P.W. and Marcopoulosi, T. 1995. Origin of the bentonite deposits of Eastern Milos, Aegean, Greece. Geological, mineralogical and geochemical evidence. Clays and Clay Minerals, 43, 63-77.

Çoban, F. 1993. Kayakent (Eskişehir) yöresinin jeolo jisi ve bölgedeki tabakalısepiyolitlerin mineralo jik incelemesi. A.Suat Erk Jeoloji Sempozyumu, 2-5 Eylül 1991, Ankara, 283-289.

Ece, Ö.I. and Çoban, F. 1990. Origin and significance of the sepiyolite beds and nodules in the Miocene lacustrine basin, Eskişehir, Turkey. In: Savaşçın, M. Y. and Eronat, A. H. (ed). International Earth Sciences Congresson Agean Regions Proceedings I, 234-245.

Erol, O. 1955. "W. Weingart 56/2, 56/4 (Sivrihisar) ve 57/1, 57/3(Ankara) paftalarının jeolojik haritası hakkında raporu"na ait korelasyon revizyonu raporu. Maden Tetkik Arama Genel Müdürlüğü Rapor No: 2473, Ankara (unpublished).

Furnes, H. 1975. Experimental palagonization of basaltic glasses of varied composition. Contributions to Mineralogy and Petrology, 50, 105-113.

Gall, Q. and Hyde, R. 1989. Analcime in lake and lake-margin sediments of the Carboniferous Rocky Brook Formation, Western Newfoundland, Canada. Sedimentology , 36, 875-887.

Gençoğlu, H., 1996. Eskişehir - Sivrihisar - Oğlakçı Köyü sepiyolit sahasının ait maden jeolojisi. Maden Tetkik Arama Genel Müdürlüğü Rapor No: 9858, 33s. Ankara (unpublished).

_____, İrkeç, T., Güngör, N., Demirhan, M. and Çokyaman, S. 1992. Lithofacial features of the Upper Sakarya section of central Anatolian Neogene basin (Sivrihisar-Günyüzü-Çeltik) and the sepiolite occurrences. 1st. International Symposium on Eastern Mediterranean Geology, 13-16 October 1992, Adana, 322-323.

_____ and _____, 1994. Ankara-Polatlı-Türktaciri sahasının maden jeolojisi. Maden Tetkik Arama Genel Müdürlüğü Rapor No: 9487, 253s. Ankara (unpublished).

Gözler, M.Z., Cevher F., Ergül E. and Asutay. H.J. 1996. Orta Sakarya ve Güneyinin jeolojisi. Maden Tetkik Arama Genel Müdürlüğü Rapor No: 9973, 87s. Ankara (unpublished).

Grim, R.E. and Güven, N. 1978. Bentonites, geology, mineralogy, properties and uses, Elsevier, Amsterdam, 256p.

Gümüşer, G. and Yalçın, H. 1998. Kelkit vadisi kuzeyindeki (Reşadiye-Yazıcık-Bereketli/Tokat) bentonit yataklarının mineralojik ve jeokimyasal incelenmesi. Yerbilimleri, 20, 91-110.

Gündoğdu, M.N.1982. Neojen yaşlı Bigadiç sedimanter baseninin jeolojik mineralojik ve jeokimyasal incelenmesi. Hacettepe Üniversitesi Fen Bilim-

leri Enstitüsü Doktora Tezi, Ankara, 386s. (unpublished).

Hardie, L. A., Smooth, J.P. and Eugster, H.P. 1978. Saline lakes and their deposits: a sedimentological approach. In Matter, A. and Tucker M.E (ed). Special Publication number 2 of the International Association of Sedimentologists, 7-41.

Hartley, A., Flint, S. and Turner, P. 1991. Analcime: a characteristic authigenic phase of Andean alluvium, northern Chile. Geological Journal, 26, 189-202.

Jones, J.B. and Segnit, E.R. 1971. The nature of opal: I.nomenclature and constituent phases. Journal of the Geological Society of Australia, 18,57-68.

Kadir, S. and Karakaş, Z. 2002. Mineralogy, chemistry and origin of halloysite, kaolinite and smectite from Miocene ignimbrites, Konya, Turkey. Neues Jahrbuch Fur Mineralogie Abhandlungen, 177, 113-132.

Karakaş, Z. 1992. Ballıhisar-İlyaspaşa (Sivrihisar-Eskişehir güneyi) yöresinin jeolojik, petrografik ve mineralojik incelenmesi. Ankara Üniversitesi Fen Bilimleri Enstitüsü Doktora Tezi, 184s, Ankara (unpublished).

_____ and Varol, B. 1993. Sivrihisar-İlyaspaşa civarı sepiyolitlerinin elektron mikroskop incelemesi, A.Suat Erk Jeoloji Sempozyumu, 2-5 Eylül 1991, Ankara, 303-310.

_____ and _____ 1994. Sivrihisar Neojen basenindeki gölsel dolomitlerin petrografisi ve oluşum koşullarının duraylı izotoplar (18O;13C) yardımıyla yorumlanması. Maden Tetkik ve Arama Dergisi, 116, 81-96.

_____ and Kadir, S. 2006. Occurrence and origin of analcime in a Neogene volcano-sedimentary lacustrine environment, Beypazarı-Çayırhan basin, Ankara, Turkey. Neues Jahrbuch fur Mineralogie Abhandlungen, 182/3, 253-264.

Kibar, M., Gökten, E., Lünel, T. and Kadıoğlu, Y.K. 1992. Sivrihisar intrüzif kompleksi ve civarının jeoloji ve petrografisi. Türkiye Jeoloji Kurultayı Bülteni, 7, 78-86.

Kulaksız, S. 1981. Sivrihisar Kuzeybatı yöresinin jeolojisi. Yerbilimleri, 8,103-124, Beytepe, Ankara.

Mariner, R.H. and Surdam, R.C. 1970. Alkalinity and formation of zeolites in saline alkaline lakes. Science, 170, 977-979.

Millot, G. 1970. Geology of clays. Translated by W.R Farrand and H.Paquet. Springer Verlag, New York, Berlin, 429p.

Moore, D. and Reynods, C. 1989. X-Ray diffraction and the identification and analysis of clay minerals. Oxford University Press, 332p.

Özbaş, Ü. 2001. Mineralogic and geochemical investigation of zeolite and related minerals of Mülk-Oğlakçı Region, Sivrihisar. Dokuz Eylül Üniversitesi Fen Bilimleri Enstitüsü Yüksek Lisans Tezi, Yök Dökümantasyon Merkezi Rapor No:109623, Ankara (unpublished).

Özen, H. and Sarıfakıoğlu, E. 2003. Sivrihisar (Eskişehir) dolayındaki volkanitlerin petrografik ve petrolojik özellikleri. 56. Türkiye Jeoloji Kurultayı Bildiri Özleri Kitabı, 14-20 Nisan 2003, Ankara, 20-21.

Özkan, O.T. and Erkalfa, H. 1977. Türkiye'de ticari bentonit killerin özellikleri ve kullanım alanlarının tesbiti. Türkiye Bilimsel ve Teknik Araştırma Kurumu Proje No: 04- 7652, 138s, Ankara (unpublished).

Paterson, E. and Swaffield, R. 1987. Thermal analysis. In: Wilson, M.J. (ed). A handbook of determinative methods in clay mineralogy, Blackie, 99-133.

Renaut, R.W. 1993. Zeolitic diagenesis of Late Quaternary fluviolacustrine sediments and associated calcrete formation in the Lake Bogoria Basin, Kenya Rift Valley. Sedimentology, 40, 271-301.

Saraç, G. 2004. Sözlü Görüşme. Maden Tetkik Arama Enstitüsü.

Schimid, R. 1981. Descriptive nomenclature and classification of pyroclastic deposits and fragments: Recommendations of the international union of geological sciences subcommission on the systematics of ıgneous rocks. Geology, 9, 41-43.

Stamatakis, M.G. 1989. Authigenic silicates and silica polymorphs in the Miocene saline-alkaline deposits of the Karlovassi basin, Samos, Greece. Economic Geology, 84, 788-798.

Streckeisen, A. L. 1976. Classification of the common ignous rocks by means of their chemical composition: a provisional attempt. Neues Jahrbuch für Mineralogie Monatshefte, H.1, 1-15.

_____, 1979. Classification and nomenclature of volcanic rocks, lamprophyres, carbonatites, and melitic rocks - recommendations and suggestions of the international union of geological sciences Subcommission on the Systematics of Igneous Rocks. Geology, 7, 331-335.

Taner, G. 2004. Sözlü Görüşme. Ankara Üniversitesi Mühendislik Fakültesi Jeoloji Mühendisliği Bölümü.

Temel, A. 2001. Post-collisional Miocene alkaline volcanism in the Oğlakçi Region, Turkey: Petrology and geochemistry. International Geology Review, 43, 640-660.

Türkmenoğlu, A., Koçyiğit, A. and Özalp, T. 1995. Kalecik-Hasayaz havzasındaki Tersiyer göl sedimanlarının jeolojisi ve kil mineralojisi. VII. Ulusal kil sempozyumu, 27-30 Eylül 1995, Ankara, 55-63.

Tucker, M. E. 1992. Sedimantary Petrology. Black-Well, Oxford, 260p.

Umut, M., Gedik, İ., Güner E., Saçlı, L. and Şen, A.M. 1991. Çifteler-Holanta (Eskişehir) Çeltik (Konya) ve dolayının jeolojisi. Maden Tetkik ve Arama Raporu No. 9204, 39s, Ankara (unpublished).

Ünlü,T., Gençoğlu,H., İrkeç, T. and Bayhan H., 1995. Turkish sepiolite deposites: A Review. In: Srivastava Rajesh K. and Chandra, R. (ed). Magmatism in relation to diverse tectonic settings, Oxford and IBH, 225-260.

Weingart, W. 1954. 56/2, 56/4 (Sivrihisar) ve 57/1, 57/3 (Ankara) paftalarının jeolojik haritası hakkında rapor. Maden Tetkik ve Arama Raporu No: 2248, Ankara (unpublished).

Yeniyol, M. 1987. Enez bentonitinin jeolojisi, mineralojisi ve oluşumu. III. Ulusl Kil Sempozyumu, 21-27 Eylül 1987, İstanbul, 123-137.

_____, 1992. Yenidoğan (Sivrihisar) sepiolit yatağının jeolojisi, mineralojisi ve oluşumu. Maden Tetkik ve Arama Dergisi, 114, 71-85.

_____, 1993. Sivrihisar'da (Eskişehir) sedimanter-diyajenetik oluşumlu yeni bir lületaşı türü. Maden Tetkik ve Arama Dergisi ,115,81-90.

Mineral Res Expl. Bull., 134, 17-26, 2007

ANTHROPOGENICAL EFFECTS ON THE PROCESSES IN THE GÖKSU DELTA, MERSİN-TURKEY

Mustafa KEÇER* and Tamer Y. DUMAN**

ABSTRACT.- The Göksu Delta, located on the Mediterranean coast in the South Anatolia, is the most significant wetland both in Turkey and Eastern Mediterranean region. The delta environments present suitable reproduction and living conditions for large numbers of continental migratory birds and aquatic species under protection. The eastern shoreline of the delta has been retreating for the last fifty years, whereas recent mouth of the delta progrades toward the gorge of the lagoon. In addition, the lagoons are filled by deposits of crevasse splay, dune and barrier islands deposits by aeolian effects. Dynamic processes in the delta environment were investigated in detail, to explain the causes of retrograding and prograding of the shoreline of the delta and to find possible solutions. According to the data obtained, the natural fluvial system, the shoreline dynamics, and the aeolian processes in the delta have been changed by the anthropogenic effects. The persistence of the variation of the shoreline will cause significant ecological disruption of the delta.

Key words: Göksu delta (Turkey), retreating shoreline, prograding shoreline, delta dynamics, geomorphological units.

INTRODUCTION

The delta environments are indispensable fertile wetlands for reproducing and existing of many fauna and flora. Therefore, the conservation of natural balance at delta environments is crucial, being natural surroundings and wild living areas (Maltby, 1991; Erdem, 1995).

The Göksu delta having a promontory shape is the most significant wetland in the Eastern Mediterranean region (Figure 1). The coastal and lagoonal environments of delta are provided reproduction and development for large numbers of flora and fauna with suitable living conditions. 450 bird species were recorded in the Göksu Delta while 352 of them are included in Ramsar list. 12 of these bird species in the Ramsar list are prone-to-extinction. 140 of these have national and 106 of them have international significance. Marine animals such as *Collinactus papidus, Caretta caretta, Cheloniamydos monchos monchos* and *Epinephelus aneus* living in the delta are under protection. In addition, 441 plant species exist in the delta. 8 of these are endemic and 32 of these are rare (Gülkal 1992; Uslu 1993).

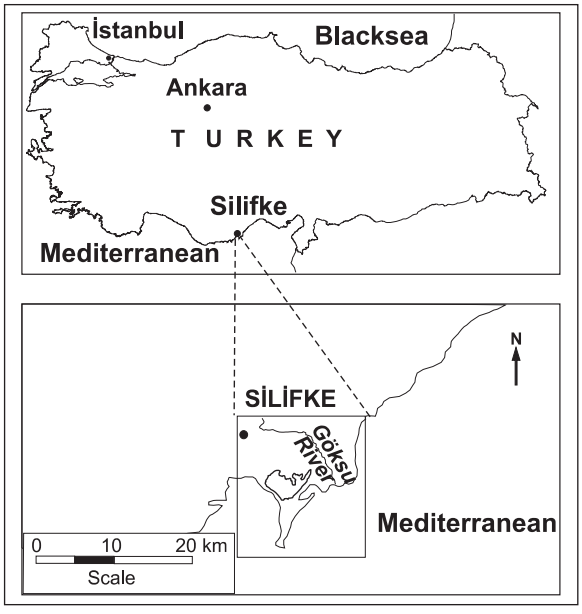

Figure 1- Location of the study area.

The Göksu delta covering an area of 165 km^2 presents a trapezoidal shape. The lithological units in the delta and its close vicinity are Devonian, Cretaceous, Oligocene and Miocene

* Kızılot Belediyesi, Manavgat / Antalya-Turkey
** Tetkik ve Arama Genel Müdürlüğü, Jeoloji Etütleri Dairesi 06520 Ankara, Turkey tduman@mta.gov.tr

clastics and carbonates (Schmidt 1961; Gökten 1976; Gedik at al., 1979; MTA, 2002). Quaternary deposits unconformably overlie these units. Large Pliocene denudational and exhumation surfaces are distinguished as main geomorphological units on the basement lithologies. During Quaternary, some fluvial incisions and slopes have been developed on the former geomorphological units in the hinterland (Keçer, 2001).

The effects of the relative sea level changes on the evolution of the delta, the changes of shoreline, the Quaternary stratigraphy along the shoreline and the isobaths of shoreline are some of the examples of the studies carried out in the Göksu Delta (Çetin at al., 1999; Ediger at al., 1993; Erinç, 1978; Erol, 1991; 1993). The formation of the Göksu delta has started 5,000 yr BP and shaped in seven stages as stated by Erol (1993). It has started forming its first stage 3,000 yr BP and acquired its most recent shape during the mid-twentieth century (Erol, 1993; Çetin at al., 1999). Okyar and Ediger (1998) investigated Quaternary units using seismic method and prepared isobaths near the delta shoreline.

This paper, as dissimilar to previous researches, intends to explain the cause of the retrograding and prograding that has reached an important grade along the shoreline of the Göksu delta. For this purpose, the amounts of shoreline variation on the Göksu delta were determined from the topographical maps produced in different times and scales. The dynamic processes existing in the recent delta environments were investigated to clarify the reason why the variation of shoreline took place. The geomorphological units were first mapped in detail to recognize the processes. Then, the relations of the geomorphological units with fluvial, marine and aeolian processes were established in the delta environments. Finally, the reasons for the retrogradation and progradation along the shoreline of the Göksu delta were evaluated based on the findings. Also, the issue how could the wetlands, which are crucial for the fauna and flora living at the delta environments, be affected by the variations of the shoreline was shed light on.

METHODS

The studies were realized in four main stages such as: (1) determining the amount of the variations along the shoreline using maps produced at different dates; (2) aerial photo (1/35 000 scale) analyses for mapping the sedimentary environments; (3) field examination of different sedimentary environments determined by aerial photographs and; (4) evaluation of the data collected.

Vertical black-and-white aerial photographs of medium scale (1/35 000) were interpreted to identify recent geomorphological units. The topographical maps at 1/25 000 scale prepared in between 1961-1995 were used to determine the variations of the shoreline of the delta. For this purpose, the maps were digitized using the on-screen methods for shoreline data input by Arc/Info geographic information system (GIS). The maps were scanned with the resolution of 350 dpi and georeferenced to the UTM coordinate system. The total root mean square (RMSE) errors were kept less than 0.005 in (=0.127 mm) which is equivalent to 3.175 m ground resolution at 1/25,000 scale. Besides, the 1/5 000 scale cadastral maps produced by local municipality were used to verify the variations along the shoreline of the eastern part of the delta. On the other hand, 1/250,000 scale topographic maps prepared in between 1945 and 1927 were utilized to locate the watercourse of the Göksu River before 1945.

RECENT VARIATIONS ALONG THE SHORELINE OF THE DELTA

The variations of shoreline of the Göksu delta in the 20th century were investigated by Çetin et al. (1999), using aerial photographs and satellite images. The researchers drafted and measured the variations amount along the shoreline around recent mouth and İnceburun. However, they only mentioned the variation of the eastern shoreline of the delta. According to these researchers, the progradation around the recent mouth of the delta occurred maximum 700 m long and cover-

ing approximately an area of 0.4 km^2 between 1951 and 1995.

In this paper, the dimensions of the retrogradation along the eastern shoreline of the delta were determined to evaluate changes of shoreline of the whole delta. According to 1/25,000 topographic maps prepared in 1961-1995, the eastern shoreline was retrograded in nearly 13 km long section under the control of the marine dynamics (Figure 2). The measured maximum retrogradation is 380 m long in this area. The spatial distribution is of 0.77 km^2 as well. At the same time, the changes along the eastern shoreline of the delta were investigated by means of the maps which were prepared at different times at 1/5,000 scale by the Municipality of Altınkum and İller Bankası. According to these cadastral maps, on 17 September 1969, 16 August 1983, 08 December 1991 and 28 August 1999, the shoreline was retrograded 170 m, 70 m and 74 m respectively and in total 314 m (Figure 3).

Using the same method, the progradation and retrogradation were re-measured for the years 1961-1995 around the former and recent mouth of the Göksu River using 1/25, 000 scale topographic maps. The whole prograded area which is

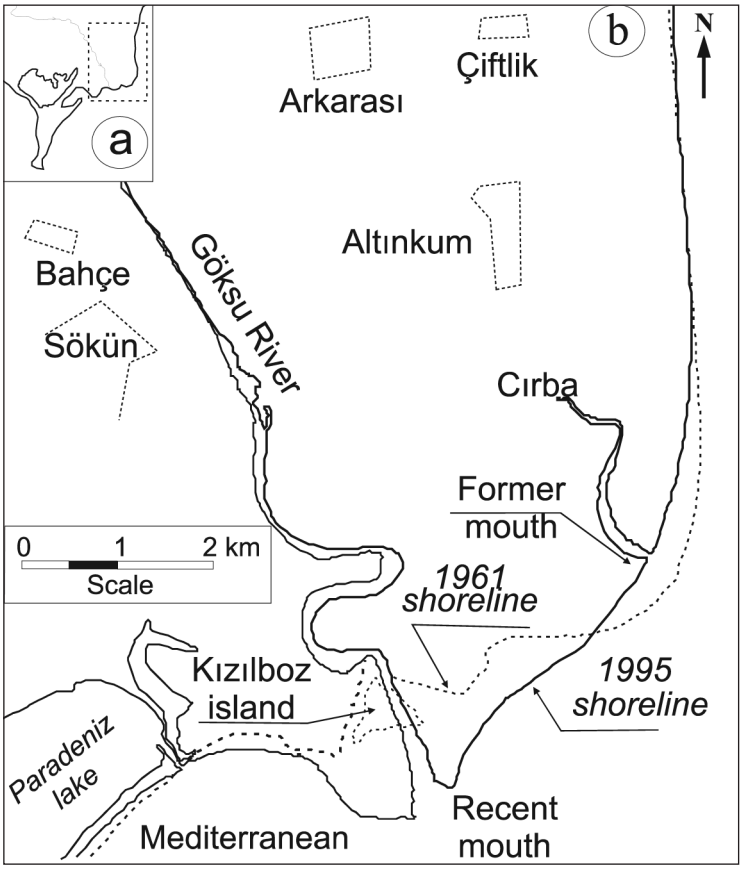

Figure 2- The variations of the shoreline in the Göksu delta. (a) The Göksu delta. (b) Progradation and retrogradation in the delta. The dotted and simple lines represent 1961 and 1995 shorelines, respectively.

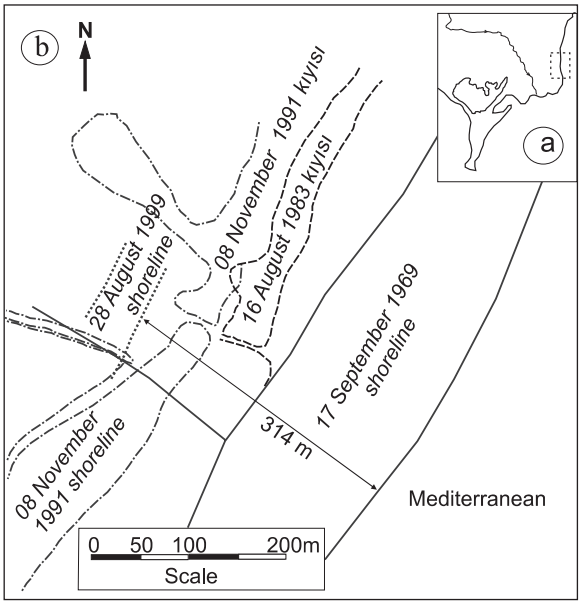

Figure 3- (a) The Göksu delta. (b) Retrogradation along eastern shoreline in the delta. The shoreline retrograding defined using 1/5 000 cadastral maps along eastern shore of the delta between 1961 and 991

effective in an area of 2.24 km^2 in the delta was identified (Figure 2). The progradation and retrogradation, which occurred during last fifty years, are found around the recent mouth and eastern shoreline of the delta. Therefore, to explain the causes of progradation and retrogradation along the shoreline of the delta, recent geomorphological formations and dynamic processes were investigated.

GEOMORPHOLOGICAL UNITS

In order to understand the recent processes in the delta, the geomorphological units present in the delta area were mapped in detail (Figure 4). These units were differentiated as five groups as fan, fluvial, aeolian, lagoonal and marine deposits. The fan deposits, which were derived from hinterland and carried by the tributary creeks to the delta, consist of semi-rounded block, pebble, sand, silt and rarely clay. The fluvial deposits formed by the Göksu River are differentiated as terrace deposits (QFt), levee deposits (QFl), flood plain deposits (QFfp), back march deposits (QFbm), ox-bow lake and cut meander deposits (QFo) and channel deposits (QFc). The aeolian deposits are dunes, which are transported from beach and former costal barrier deposits. Lagoonal and marine deposits are quite complicated at the Göksu delta. The main units of these are coastal plain deposits (QMcf), marine beach deposits (QMb), former coastal barrier deposits (QMfcb), lagoonal coastal plain deposits (QMlc), lagoonal swamp deposits (QMlm) and former lagoon deposits (QMfl).

The geomorphological units mapped in the delta have been formed as a result of the fluvial, marine and aeolian processes. The active processes that continue on the delta can be transformed to ineffective processes. In this situation, the dynamic processes are exchanged for another and the environments were transmitted to effect of a new dynamic process. So, main erosional and depositional processes of fluvial, marine aeolian, which have significance effects at the delta, are explained below.

Fluvial depositional and erosional processes

The Göksu River is the main factor for the formations in the delta environments. The river performs its basic functions (depositional elements) between levees located on both flanks of the river. The flat-lying levees parallel to the river are asymmetric natural levees. Except for the times of flood, the Göksu River maintains its erosional and depositional processes between the natural levees. From Silifke to the shoreline, the levees with abandoned beds and ox-bows in between are situated (Figures 4 and 5). These relicts of the former beds are observed between the two levees of the Göksu River, getting wider toward the Mediterranean Sea (Figure 4). During the floods, the Göksu River tears the natural levees and transports fine material to the flood plain,

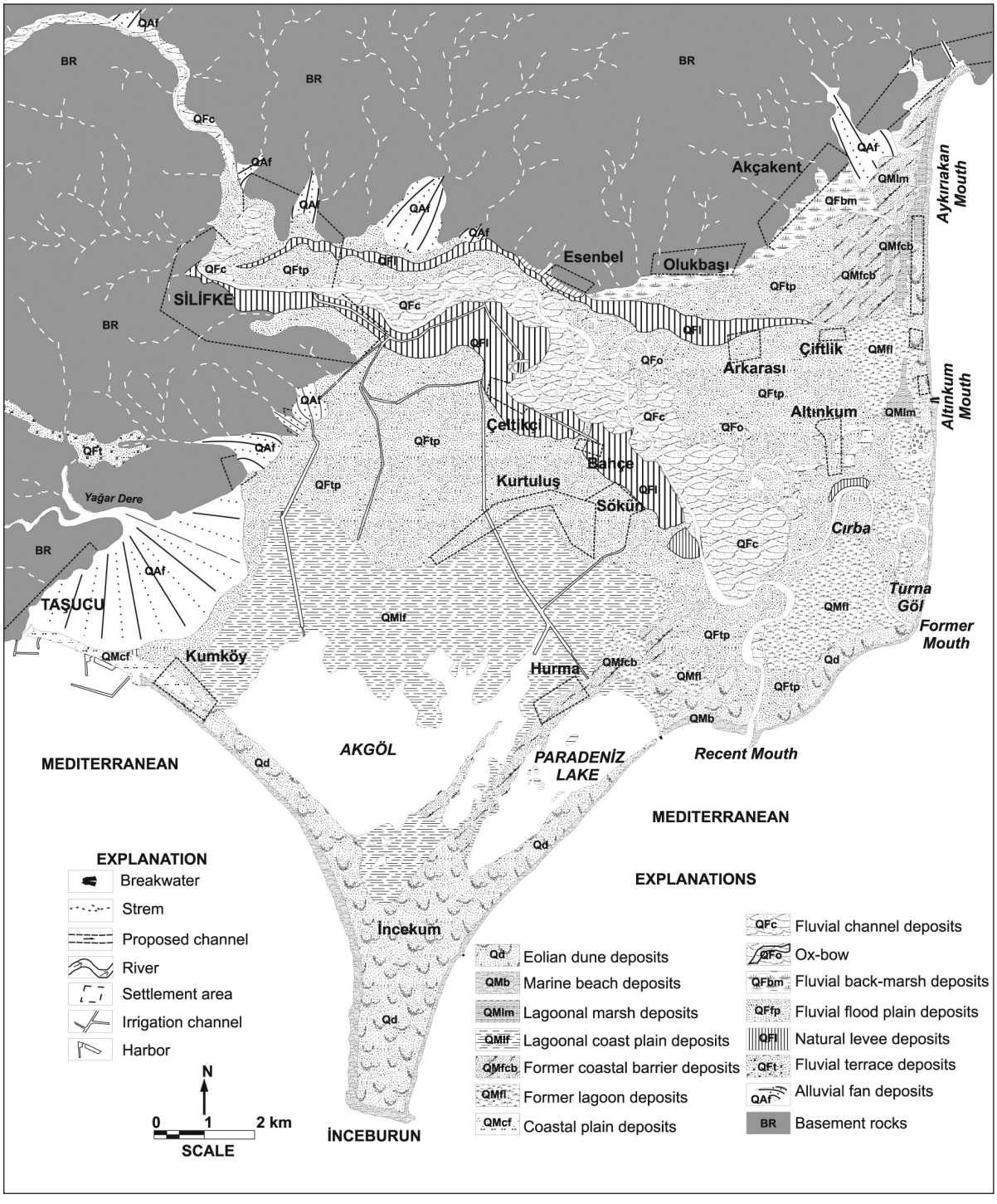

Figure 4- The map of the Quaternary deposits in the Göksu delta

lagoonal costal barrier, former and recent lagoons by the crevasse splay. Small size deposit fans with a smooth morphology were formed as a result of this process. The dendritic pattern drainage such as gully is observed on these fans.

Marine depositional and erosional processes

The fluvial material carried by the Göksu River was transported and deposited by the marine activities from both flanks of the mouth as the depositional marine units. Frontal-coast barriers or barrier islands and mouth barrier deposition units lying parallel to the shore were formed as a result of this process. There are two diverse barrier islands that belong to recent and former sea level at the delta.

The old ones have formed depending on former sea level rising and drowning. The most evident barrier island was divided into three parts by two inlets at Çiftlik region (Figure 4). The other barrier island of the same period was situated between Paradeniz and Akgöl lagoons, like a coastal cord. This barrier island lies parallel to the coast between the Göksu River and İncekum and is separated by an inlet, at the northeast of Paradeniz. Another old barrier island having a concave shape and lying between Kumköy and İncekum formed as a result of the transportation of the material by Yağar Stream in SE direction. The younger barrier island was formed by the current sea level as a continuation of the beach. It is flat and leans against the former barrier island. It is discriminated from the former ones by having coastal dunes.

The marine erosional units are gorges between barrier islands, escarpments on the shoreline, erosions along the beach of the storm waves, and the destructive effect of marine currents on the breakwater roots.

Aeolian depositional and erosional processes

The sands, which belong of the former and younger barrier islands and beach in the delta, have formed the coastal dunes by moving in two directions with aeolian effects. The movement direction of the dune between the Cırba Mouth and Kumköy is from southwest to northeast while the other is from northeast to southwest (Figure 4). This area extends from Aykırıakan to the abandoned beds located around the east of Altınkum. The source for coastal dunes is former coastal barriers and current beach sands. The costal dunes in the direction of the recent lagoon, former lagoon and back-marsh have steep slopes, but toward the sea they have gentler slopes. Some of these dunes are active, while the other ones are fossilized.

ANTHROPOGENIC EFFECTS ON THE NATURAL DYNAMICS

Corresponding to the abandoned beds and ox-bows, the Göksu River flowed between Çiftlik and Cırba, and drained into Mediterranean Sea from the eastern shore of the delta. However, the recent mouth of the Göksu River is located around Paradeniz Lake in the south. The variations of the Göksu River mouth occurred about 1950s have been determined from the topographic maps printed between 1927 and 1995 by the General Headquarter for Mapping of the Turkish Army (HGK). The Göksu River drained into the Mediterranean Sea from Cırba (former) mouth based on the 1/250 000 scale topographic maps printed in 1927 and 1945. But, according to the 1/25 000 scale maps printed from 1961 on and aerial photographs taken from 1956 on the Göksu River drains its waters into the Mediterranean Sea from the new mouth close to the Paradeniz Lake.

According to the geomorphological units that were investigated in detail and by recent dyna-

mics processes, the changes of the river mouth did not occur naturally. In the delta, the Göksu River flowed between the levees located its either two side, which is obvious from the abandoned channel and ox-bow lakes. There is no other geomorphological data showing that the Göksu River flowed outside of the natural levees.

Although the date is not definitely known the Göksu River was artificially diverted to the new mouth from the its former mouth (Cırba). According to the local people, this diversion of the Göksu River mouth was made in 1952. Another possibility for this diversion might be that when the river was forced to flow out of its original bed and forced to flowed linearly by human activity from the northeast of Sökün in 1955 (Figure 4).

This diversion that is made in 1950s caused a number of changes in the delta environments. The river tears the natural levees in the flood seasons because of the thalweg of the river increased due to the forcing to linear flow of the river for a 4.5 km distance to southwest from former mouth. At the new progradation point, a new asymmetric delta lobe formation began with the sediments that are transported by increased energy and a higher flow rate of the river in the SW direction (Figure 5). The geometry of the lobe is also obvious on the bathymetric chart (Okyar and Ediger, 1998) of the delta area. During these processes, Kızılboz Island existing near the recent mouth was connected to the coast and a new coastal barrier has been formed at the shore.

In the event that persistence of the lobe formation will cause a risk to close of the mouth of the Paradeniz lagoon. If this lobe formation maintains, the inlet of the Akgöl located more to northeast, as a former lagoon and temporary lake, will be either closed or displaced as well. This situation will cause significant ecological degradations and decreasing the effect of the sea on the Paradeniz lagoon and Akgöl.

The coastline is being changed by SW trending marine erosion, which become predominant by ceasing the fluvial transportation at the former progradation area (Cırba mouth, Turna Lake, Aliağa Lake, and the coast to the breakwater at North). In this area, under the control of marine dynamics, the shoreline has retrograded in the last three decades along approximately 13 km part of the shore. In the event that preventative measures are not taken, the progradation will reach 1.2 km close to Altınkum and up to the linear line where is from the 2 m altitude point located eastern side of the river mouth to Ayıkıran.

On the other hand, the vegetation of the barrier islands and dunes has been destroyed by human activity and by excavations for taking aggregates. Because of these, the barrier islands, which have very important role in forming and keeping position of the lagoons, have been damaged by aeolian erosion. The materials moving with aeolian effects from the barrier islands and dunes have been deposited in the former lagoons. In case of flood of the Göksu River forced to linear flow, the conduit crevasse has been transported the materials to the former lagoons. The wetlands are being filled by these materials transported and transformed into terrestrial area.

The beaches are protected by means of the barrier islands. Destructions of the barrier islands by aeolian effects result in damage of beach sand by the waves. In addition, the draining channels constructed during the reformation in the delta flow into Akgöl and Paradeniz Lagoon. The sediments and chemical waste derived from agricultural areas are transported by the draining channels to these lakes.

DISCUSSION AND CONCLUSION

The effective directions of the marine current are different at the shore of the Göksu Delta (Okyar and Ediger, 1998). The dominant marine currents are clockwise at the eastern shore of İnceburun, while they are counterclockwise at the

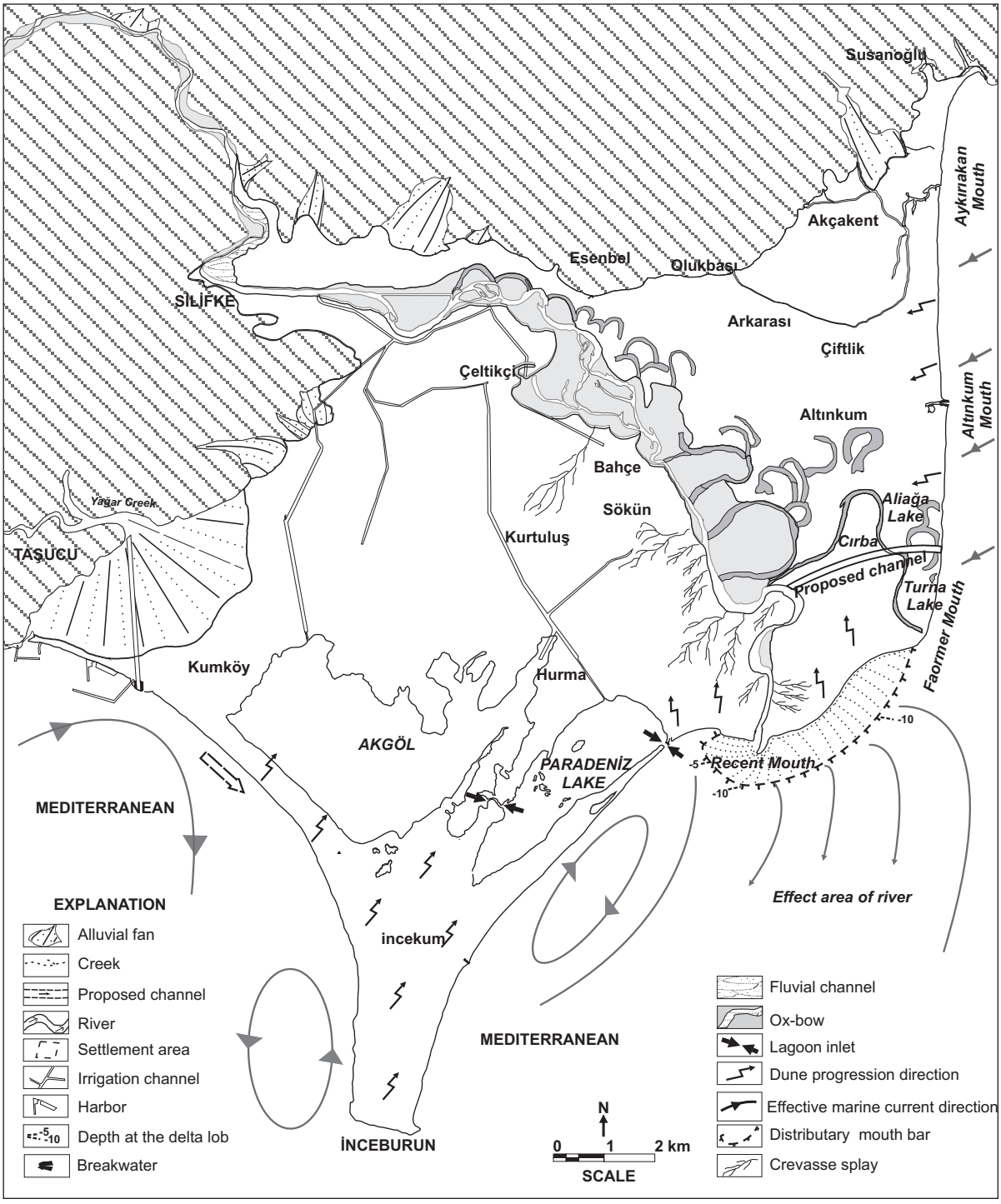

Figure 5- The natural dynamics processes in the Göksu delta. Marine currents directions from Okyar and Ediger (1998)

western shore of the delta (Figure 5). The dominant currents at the eastern and southern shore are toward southwest and clockwise parallel to the shore, respectively. The Göksu River is the source of the dynamics of the fluvial erosion and deposition in the delta environments. The river continues its activity within the bed fan-shaped widening towards southeast at the delta (Figure 4).

The Göksu River and the currents of shore have basic agents for developing unique shape and natural balance of the Göksu Delta. The Göksu River was flowed within the levees towards southeast during its natural process. This is also evident on traces left by the river flowed between natural levees (Figure 4). The river transported the sediments to the eastern shore of the delta during its natural process. These transported sediments were processed by southwest marine currents and formed barrier islands. The barrier islands that formed in different times were played significant role to shape and form both Paradeniz Lake and İnceburun. The reverse currents each side of the İnceburun was simultaneously assisted to gain the special feature of the delta as well. This system has been destroyed due to anthropogenic interference to the natural processes of the Göksu River bed. The eastern shoreline of the delta has been retreated more then 350 m while the shoreline has been propagated about 700 m around recent mouth of the river. The persisting of the propagation 15 m/year in average will be resulted in a risk to close the inlet of the Paradeniz lagoon.

It is now accepted that the delta environments is crucial for many fauna and flora. In this context, taking into consideration of protecting the shore, marshy areas and agricultural places, land use planning studies have been carried out by local government. The status of first-degree natural preservation of the delta area was declared.

Besides the protecting and planning studies of the delta, the rebuilding of the natural equilibrium at the delta is indispensable condition. For this reason, the natural dynamics processes of the delta should be again provided. For this purpose, the Göksu River should be taken on an artificial channel starting from Cırba segregation and reaching to the sea at Aliaga Lake region and flowing towards the former delta progradation of the river should be again provided (Figure 4). So, this region of the delta becomes from retrogradation into progradation in character by its natural processes. Therefore, recent mouth can be prevented because of the deposition at the current mouth. Also, the formation of the lobe will be ended, developing close the mouth of the Paradeniz Lagoon. In addition, transportations of the materials to the lagoons by crevasse splays will be reduced and filling of the lagoons by these deposits will be ended.

The bed of the Göksu River, which will be abandoned southern from starting point of the artificial cannel, can be transformed into wetlands being the water of river under the control and can be used as a 4 km-length fish trap. Bringing to a stop of taking aggregate material from the beaches and barrier islands and growing plants suitable for the ecosystem on the dunes can be also provided stability.

ACKNOWLEDGEMENTS

This work is done as part of 'Delta of the Goksu Project' supported by The General Directorate of Mineral Research and Exploration (MTA). The authors would like to gratefully acknowledge the support provided by MTA. We also thank Mustafa Gedik who provide cadastral map from Municipality of Arkum.

REFERENCES

Çetin, H., Bal, Y. and Demirkol, C., 1999. Engineering and environmental effects of coastline changes in Turkey, northeastern Mediterranean. Environmental and Engineering Geosciences, Vol. 3 pp. 315-330.

Ediger, V., Okyar, M. and Ergin, M., 1993. Seismic stratigraphy of the fault controlled submarine canyon/valley system on the shelf and upper slope of Anamur Bay, northeastern Mediterranean Sea. Mar. Geol., 115, 129-142.

Erdem, O. 1995 Turkey's bird paradises. Green Series: 5, Publication of the Ministry of Environment, General Directorate of Environmental Protection, Ankara, Turkey.

Erinç, S. 1978. Changes in physical environments in Turkey since the end of the last glacial In: (W.C. Brice, Ed.), The environmental History of the Near and Middle East since the last ice Age Academic press, London, pp. 87-108.

Erol, O. 1991. Impacts of sea-level rise on Turkey, International Sea-Level Rise Studies Project. Institute of Marine and Coastal Sciences Rutgers-The State University of New Jersey, New Brunswick, USA.

_____, 1993. Türkiye kıyılarındaki bağıl deniz düzeyi değişmeleri ve bunun Göksu Deltası ile diğer deltaların evrimine etkisi. Uluslararası Göksu Deltası Çevresel Kalkınma Semineri Bildiri Metinleri, Doğal Hayat Koruma Derneği, Istanbul.

Gedik, A., Birgili, S., Yılmaz, H. and Yoldaş, R. 1979. Mut-Ermenek-Silifke yöresinin jeolojisi ve petrol olanakları. Türkiye Jeol. Kur. Bült. 22, 7-26.

Gökten, E. 1976. Silifke yöresinin temel kaya birimleri ve Miyosen stratigrafisi. Türkiye Jeol. Kur. Bült. 19, 117-126.

Gülkal, O. 1992. Göksu Deltası'nın doğal ve kültürel potansiyelinin belirlenmesi ve kullanımlar yönünden değerlendirilmesi. C.U. Fen Bilimleri Enst. Yüksek Lisans tezi (unpublished) Adana-Türkiye.

Keçer, M. 2001. Göksu Deltası'nın (Mersin) jeomor folojik evrimi ve güncel akarsu-deniz-rüzgar süreçlerinin kıyı çizgisinde yaptığı değişiklikler. MTA Raporu No: 10468. (unpublished) Ankara.

Maltby, E. 1991. Wetland management goals: wise use and conservation. Landscape and Urban Planning, 20, 9-18.

MTA. 2002. 1/500, 000 ölçekli Türkiye Jeoloji Haritaları, Adana Paftası. Maden Tetkik ve Arama Genel Müdürlüğü yayınları. Ankara, Türkiye

Okyar, M. and Ediger, V. 1998. Göksu Deltası'nın Kuvaterner jeolojisinin sismik yöntemlerle incelenmesi alt projesi sonuç raporu. ODTU Deniz Bilimleri Enst. Erdemli-İçel.

Uslu, T. 1993. Göksu Delta'sında kıyı kumul yönetimi. Uluslararası Göksu Delta'sı çevresel kalkınma semineri bildiri metinleri. Doğal Hayatı Koruma Cemiyeti-İstanbul.

Mineral Res Expl. Bull., 134, 27-34, 2007

THE FIRST FINDINGS ON THE ORIGIN OF ALVEOLAR DISINTEGRATION AT THE WESTERN SHORES OF GELİBOLU PENINSULA

A. Evren ERGİNAL*, Ahmet GÖNÜZ*, Mustafa BOZCU**, A. Suat ATEŞ*** and Ziya S. ÇETİNER**

ABSTRACT.- Various specific disintegration types, characterized by alveolar disintegration, were observed in Cape Büyükkemikli, at the northern side of Suvla Bay and western side of Gelibolu Peninsula. Field observations and analytical data indicate that alveolar disintegration, which developed over Oligocene sandstones, is dominant at carbonate-cemented sandstones, with fine to medium texture and rich in biotite and plagioclase. Alveolisation ideally develops over the surfaces of sandstone layers, which are dipping towards the sea with an angle of 33-40°. Furthermore, it is understood that disintegraton over sandstone is related to micropore and microfracture zones and supported by the biogenic origined formations along the intratidal zone. Salt disintegration is effective within the wave wash zone as a result of evaporation conditions during the periods of May-June. Besides, ellipsoidal disintegration cells and tafoni formations are abundant over frontal walls, which receive the impact of south sector winds with right angle. The edges of polygonal fracture zones, hardened by iron oxide infillings delimits alveolisation.

Key words: Alveol, salt disintegration, biogenic disintegration, intratidal zone, Gelibolu Peninsula.

INTRODUCTION

Alveolar disintegration is a technical term used for honeycomb weathering patterns developed especially over sandstones, depending on wind erosion, exfoliation, freezing-thawing, salt disintegration and precipitation. This specific disintegration process, dominated over sandstones, is represented by honeycomb weathering pores and their 1-m or larger equivalents which are known as tafoni formations, formed under the control of geomorpological, geological, climatological and especially at the shore regions by hydrodynamical and biological factors. The first observations related to their formations were done by Darwin (1839) and Dana (1849) in Australia, and a variety of definitions such as honeycomb weathering, stone lattice rather than alveolar disintegration were made. The definitions and theories were studied in detail by Mustoe (1982), Turkington and Phillips (2004) and Turkington and Paradise (2005).

According to previous studies, alveolar disintegration may develop over different rock types such as diorite, tuff, agglomerate and sandstone, under different climatic conditions. There are so many examples of alveolar disintegration over sandstone as it is the most frequent and important (Scherber, 1927; Bouchart, 1930; Rondeau, 1965; Mustoe, 1982; Kelletat, 1980; Mellor el al., 1997; McBride and Picard, 2004; Turkington and Paradise, 2005). The most accepted idea so far is that the alveolisation occurs on the control of salt disintegration (Evans, 1970; Bradley et al, 1978; Mc Greevy, 1985; Cooke et al, 1993). Yet there is debate over the origin of alveolar disintegration, there is still no study on Turkish shores related to this subject.

* Çanakkale Onsekiz Mart Üniversitesi, Fen-Edebiyat Fakültesi, Coğrafya Bölümü, Terzioğlu Kampüsü, Çanakkale. aerginal@comu.edu.tr - ahmetgonuz2@yahoo.com

** Çanakkale Onsekiz Mart Üniversitesi, Mühendislik-Mimarlık Fakültesi, Jeoloji Mühendisliği Bölümü, Terzioğlu Kampüsü, Çanakkale. mbozcu@comu.edu.tr; ziyac@comu.edu.tr

*** Çanakkale Onsekiz Mart Üniversitesi, Su Ürünleri Fakültesi, Temel Bilimler Bölümü, Terzioğlu Kampüsü, Çanakkale. asuatates@yahoo.com

At this study, alveolar disintegration observed at the Cape Büyükkemikli, located at the northern side of the Suvla Bay and western side of the Gelibolu Peninsula, were considered with a multidisciplinary approach. Alveols and tafonis at the alveolar disintegration zones (Figure 1) over

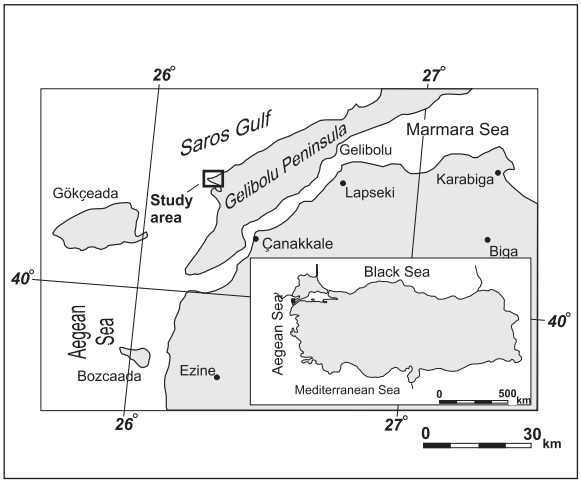

Figure 1- Location map of study area

Oligocene sandstones cover a wide region from the shore line to 15-m-altitude. Over the region, where alveols different in shape and size developed, the morphometric properties of alveols and tafonis, petrographical features of sandstones, and the systematics of joint and fractures over sandstones were studied. Besides, it was attempted to determine the colonial features of macroendolitic and surface fauna, which have settled into alveol and tafoni pores, considering bioerosion arising from the relation between the microscopic epilite and endolites as the primary producers of bioerosional community. The study was concentrated on the relation of alveolar disintegration to sea water and salt brine, the impact of climatic components over the sandstone disintegration, the density of cyanobacteria over sandstone, and the effect of various physical and chemical factors such as temperature, pH and salinity over the disintegration process. The study includes the preliminary results of ongoing research about the geomorphological, petrographical, structural, biological and sea water/salt brine which are effective on the disintegration developing on the study area.

LOCAL GEOLOGICAL AND GEOMORPHOLOGICAL FEATURES OF STUDY AREA

Eocene-Oligocene units have been distributed over the study area, geology of which was previously studied by Önem (1974) and Sümengen and Terlemez (1991) and the surrounding area. Sandstones, having wide outcrops in the study area with alveolar disintegration development, were evaluated within the Korudağ formation by Kellog (1973), and are impure yellow colored, laminated, with low to medium thickness. Strike of layers is generally N50E, and dip is 38-50 SE (Plate I, Figure 1). Orthogonal and polygonal fracture systems, in which resistant crusts were developed due to calcite infillings and especially iron aggregation, are generally NE-SW and NW-SE directed (Plate I, Figure 2). Sandstone overlies massive silty-mudstone, described as Keşan formation by Gökçen (1967) and Kellog (1973), conformably. The geomorphology of study area is generally represented by low plateaus slightly descending generally towards western and southwestern direction, and broad valleys developed over clayey and silty units and small bays. Cape Büyükkemikli, composed of mainly sandstones, forms an extension of the plateau, which descends from Karakol Mountain (141 m) at the northwestern part of region towards southwestern direction and mainly composed by Upper Eocene and Oligocene sandstones, limestones, and siltstones. NW trending hillsides of NE-SW directed plateau have slopes with 20°-90°. Together with this, general slope arises 50°.

In the area, steep-cliff type shore is dominant, and small shores with siltstone ovarlain were developed. Wave action is effective over the layer as their slopes are towards southeastern direction in Cape Büyükkemikli. Thus, abrasion platforms are widely distributed in front of cliffs.

METHOD OF STUDY

Sandstones with and without alveolar disintegration were sampled to introduce driving factors for the alveolar disintegration and its origin. Standart thin sections of samples were prepared and these were classified according to Folk (1970) classification. By studying EDS (Energy Dispersive X-Ray Spectroscopy), and SEM (Scanning Electron Microscopy) analyses, mineralogical composition, cement type and abundance, and element composition effective on disintegration were studied. Furthermore, the systematic and geometry of fractures over the sandstones in the study area were examined in 22 different sampling sites. The biological species observed in the shoreline have been grouped based on their act on the shoreline morphology, and their impacts on disintegration were evaluated. The impact of sea water composition on disintegration was evaluated by the analysis of ICP-AES (Inductively Coupled Plasma - Atomic Emission Spectroscopy) from sea water samples.

Table 1- Geochemical analysis results of seawater from the section of alveolar disintegration in the study area

Parameter	Value
T(˚C)	18.3
EC (µS/cm)	48300
pH	8.9
TDS (mg/kg)	29700
Na^{+} (mg/kg)	6915.7
K^{+} (mg/kg)	680.4
Ca^{++} (mg/kg)	403.8
Mg^{++} (mg/kg)	1095.3
Cl^{-} (mg/kg)	15862.7
SO_4^{--} (mg/kg)	2469.7

PRELIMINARY FINDINGS

Preliminary findings obtained from the study, which presents the alveolar disintegration at the study area and its promoting factors are described below

Impact of petrographic features of sandstones on alveolar disintegration

Sandstone, over which alveolar disintegration has developed, are carbonate-cemented, yellowish quartzarenite and subgreywacke, with clay and chlorite matrix, according to Folk (1970) classification. They have abundant quartz and plagioclase with minor amounts of biotite and muscovite and show a fine-medium texture with abundant serpentine, chert and metamorphic rock fragments. The impact of rock over the disintegration especially depends on its clay, plagioclase and biotite mineral abundances. As it can be concluded from the comparison of thin sections of sandstone samples with and without alveolisation, the increase of plagioclase and biotite abundance in sandstone promotes the development of alveolar disintegration. Sandstone with dominant alveolar disintegration is carbonate-cemented, fine-grained and named as quartzarenite. Rock is rich in plagioclase and has granular texture (Plate I, Figure 3). In sandstones with no alveolar disintegration, rounded or subrounded quartz grains with undulose extinction are abundant (Plate I, Figure 4). Micas are composed of muscovite cement is carbonate and rock is named as micaceous subgreywacke.

Development of alveolar disintegration is expecially related with mineral grains in sandstones and carbonate cement binding rock fragments. This situation can also be concluded from EDS analysis of rock samples. Alveolar disintegration is abundant on sandstones with high Ca^{++} content (Table 2a). Results of elemental analysis indicate the existence of iron and magnesium which are reduceing factors of dissolution. Thus in sandstones with minor Ca^{++} and abundant Mg^{++} ve Fe^{++}, the alveolisation either is stopped or is very limited (Table 2b).

When SEM images of rock samples were studied, microporosity and microfracture compo-

Table 2-a-b EPS analysis of rock samples

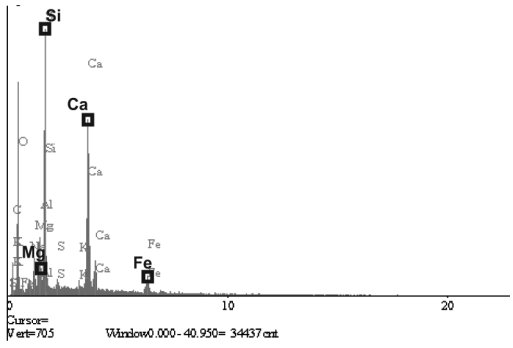

Elt.	Line	Intensity (c/s)	Conc	
C	Ka	8.42	0.000	wt.%
O	Ka	61.55	0.000	wt.%
Na	Ka	5.03	2.121	wt.%
Mg	Ka	11.65	3.644	wt.%
Al	Ka	26.15	7.454	wt.%
Si	Ka	121.04	34.978	wt.%
S	Ka	4.44	1.480	wt.%
K	Ka	2.84	0.875	wt.%
Ca	Ka	126.33	40.589	wt.%
Fe	Ka	12.30	8.859	wt.%
			100.000	wt.% Total

a

15:56:15PM 24-Apr-2006

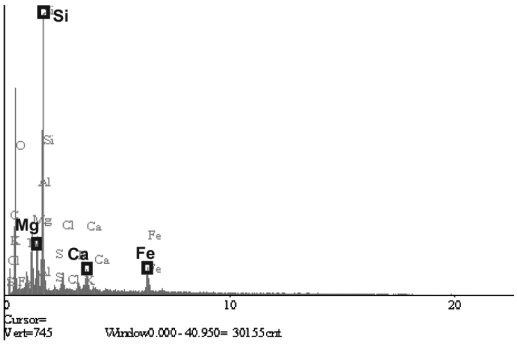

Elt.	Line	Intensity (c/s)	Conc	
C	Ka	2.24	0.000	wt.%
O	Ka	59.66	0.000	wt.%
Na	Ka	7.70	3.527	wt.%
Mg	Ka	23.86	8.529	wt.%
Al	Ka	25.40	9.019	wt.%
Si	Ka	130.05	47.651	wt.%
S	Ka	1.91	0.877	wt.%
Cl	Ka	13.42	5.883	wt.%
K	Ka	5.33	2.297	wt.%
Ca	Ka	15.79	6.935	wt.%
Fe	Ka	17.98	15.280	wt.%
			100.000	wt.% Total

b

15:55:42PM 24-Apr-2006

sition of sandstones are seen also effective over the progress. When SEM images of sandstones with dominant alveolar disintegration were examined, it can be observed that rock is rich in microporosity and microfractures (Plate II, Figure 1). Pore size is generally around 50-100 μm and fractures connecting the ellipsoidal pores have length varying between 100-400 μm. Sand stones without alveolisation, on the other hand, are rich in micaceous flakes and have dense carbonate cement (Plate II, Figure 2).

Relation of sea water and brine salt with alveolar disintegration

Relation of alveolar disintegration and crystallized salt produced under the strong evaporation conditions in dry season which creat a pressure on the rock surface and alveol walls is the most accepted theory (Evans, 1970; Bradley et al., 1978; Mc Greevy, 1985; Cooke et al., 1993; Rodriguez-Navarro et al., 1999). Observations in the study area indicate that in the dry season (July-August 2006) sea water spilled with waves can reach upto 5 m height. Indeed, within the mentioned altitudes on the sandstone beds, in the fractures and alveols salt concentration is observed. In order to explain brine salt during the disintegration, some geochemical analyses were carried out.

Results of ICP analysis of the sample recovered from sea water indicate that NaCl known as hygroscopic, is the main component which is transported by waves and may cause important chemical reactions (Andrews et al., 2004). Results of ICP analysis are shown in table I regarding development of alveolar disintegration, the following reaction can be proposed:

$$H_2SO_4\ (aer) + NaCl\ (aer) \rightarrow HCl\ (g) + NaHSO_4$$

According to this, sea water may affect aerosol formation in various degrees. This condition will create an acidic environment in which disintegration rate increases. In order to prove the reaction, PHREEQC software (Parkhurst and Ap-

pello, 1999) is used, by this way, distribution and concentration of chemical substances are determined. Calculations are performed on the basis of physical and chemical parameters such as T (°C), pH and average major element concentrations. As a result, Na^+ ve Cl^- are found as both seperate ions and ion couples (NaCl°) and in that form they are the main component of the reaction which causes the formation of acidic media which results the alveolar disintegration.

Morphological and morphometric features of alveolar disintegration types

In the study area, many samples which are discussed in the literature are observed (rounded, ellipsoidal, turtleback, tendril, tafoni, etc.).

Among the formed structures, ellipsoidal disintegration cells under the control of rounded, subfractured systems are dominant. However, besides the petrographic features of sandstones, different factors such as biogenic impacts, layer slope, salt disintegration, and wind condition and lichen disintegration play important role on the distribution of these structures and their dimensional properties. For this reason, from 4 different locations, selected from a line between sea level and 15 m height of Cape Büyükkemikli, 50 measurements from alveols were made considering the depth, width and length of alveols.

The first two measurement site is located in intratidal zone within a 0-1 m altitude range. At the first of these sites, the measurements from sandstone layers with N60E strike and 37° SE dip has given 15-65 mm length, 15-50 mm width, and 10-45 mm depth. Rounded and ellipsoidal alveols are dominant and at the regions where *Semibalanus balanoides* and *Littorina neritoides* species lived in vast amounts, alveol walls were enlarged and their morphology is deformed as a result of biogenic weathering (Plate II, Figure 3).

Another measurement from the same altitude range is among the sandstone layers with no difference at petrographical or structural features. The major difference here is the increase at the alveol sizes. This difference arise from the density increase at the colonies of Balanus over sandstones and their major nutrients, blue-green algae. At this site, alveol walls and heels vastly consists *Enteromorpha* sp., *Rhizoclonium tortuosum* and *Cladophora sericea* from green algae, *Calotrix confervicola* from blue-green algae as globular forms, and *Amphora* sp. and *Navicula* sp. from diatoms. The measurements indicate that the long axes vary between 3.5-10 cm, whereas width and depth change between 2.5-8 cm and 1.5-6 cm, respectively. Especially, the increase in depth and intergrowth structure (funnel) are morphological features defining locally-formed alveols. However, the major role for such formations is the disintegration impact resulted from the crystallization of salt coming from sea water and deposited into alveol heel and walls during dry season. For this reason, alveol walls get thinner and get perforated or coalesced within time (Plate II, Figures 4 and 5). Marine species such as *Semibalanus balanoides* (Linnaeus, 1758), *Euraphia depressa*, *Euraphia depressa* (Poli, 1795), and *Littorina neritoides* as a member of gastropoda family (Linnaeus, 1758), existing in the varying sizes of alveols, promote alveolisation biogenically, but, deform the morphology of structures (Plate II, Figure 6).

The third measurement point is located on the N70E trending, 30-38 southeast dipping sandstone beds 1-5-m above the sea level. In this section dimensions of the disintegration cells varies as follows: length 2 mm - 8.5 mm, width 1.5 mm- 6 mm and depth 1 mm - 4 mm (Plate III, Figure 1). In the parts where fracture systems intersected and frontal walls directly effected by south west winds; streched disintegration cells are abundant (Plate III, Figure 2). Tafoni formations were observed along the layers having the less than 20 cm thiknesses (Plate III, Figure 3). In addition, near the systematic alveol cavities; atleast one side open, low and thinner walled alveols (tendrils) (Plate III, Figure 4) and so called turtleback alveolar disintegration speci-

mens (Plate IV, Figure 5) were partly observed on the surfaces of sandstones which are being weathered.

The last measurement site selected to evaluate the relation with alveolar disintegration is located in the region at the topmost part of Cape Büyükkemikli (15-h height) where lichen community is available. The results of measurements from sandstone layers with N85E strike and 32° dip, vary as 3.5-1 mm length, 2.5-1 mm width and 3-11 m depth. These rounded and very small alveolar cells were vastly filled with Xantoria species (Plate III, Figure 6).

DISCUSSIONS AND CONCLUSIONS

The results of petrographical and physico-chemical analyses may lead the following conclusions.

In the study area, alveolar disintegration is related to the mineralogical composition, texture and presence of carbonate cement and its compaction degree in the sandstones. Alveolar is developed in fine-grained, carbonate-cemented, plagioclase and biotite-rich sandstones.

Elemental composition of sandstone is an important parameter of alveolar disintegration. Alveolar disintegration cannot be developed or is weakly developed in sandstones, which have poor Ca^{++} content and relatively rich Mg^{++} and Fe^{+} content.

The micropore and microfracture content of sandstone are important parameters which are effecting the development of disintegration. On the other hand, polygonal fracture systems delimit the lateral development of the disintegration, because mostly they are hardened by iron oxide infillings.

In the study area, disturbed and wet samples were recovered from the alveolar cavities which are found in the intratidal zones. Within these samples, *Rhizoclonium tortuosum* and *Cladophora sericea* belonging to green algae group are vastly observed, fibrous *Calotrix confervicola* and globular form of *Chorooccus minor*, belonging to blue-green algae and *Amphora* sp. and *Navicula* sp. from diatom group are intensely observed. These algaes are nutrients of some groups of gastropoda. *Enteromorpha* sp. from green algae is vastly observed in wet rocks and their peripherals. The vast occurence of patella and balanus species on the rock surfaces, salt content of the some dried alveols, within which blue-green algaes changed into black and fill the fractures in this small zone, sea organisms leaves their excrements and organic acid, as a result, sandstone are disintegrated. In addition to that, *Semibalanus balanoides*, *Euraphia depressa*, gastropoda *Littorina neritoides* as rock borrowers which are fed on this algae are observed on sandstone surfaces. These organisms have the ability to disintegrate carbonaceous rocks and sandstones, because they have carbonate shells or radula. In the study area, disintegration occurs effectively within 1 m below the sea level.

200 measurements of the alveols show that their dimensions vary between cm to dm. They are generally rounded in form, fractural disintegration cells contain ellipsoidal forms.

Salt disintegration in the dry season between May and August in the study area. As a result of salt disintegration, increase in size of alveols, thinning of alveol walls and connical development of alveols, rapid evaporation of salt solution due to wind. Therefore, in the layers, which are taking wind directly at right angles, the salt disintegration is more effective and sea water composition and especially NaCl couples effect the disintegration. Furthermore, for better understanding of disintegration process, pH, salinity, and excremence of marine organisms and acids with more samples will be evaluated and presented in a future study.

Manuscript received October,30,2006

REFERENCES

Andrews, J.E., Brimblecombe, P., Jickells, T.D., Liss, P.S., and Reid, B.J. 2004. An Introduction to Environmental Chemistry. Blackwell Science, Oxford, U.K, 296p.

Bouchart, J. 1930. Le probleme des "taffoni" de Corse el l'érosion alvéolaire. Revue de Géographie Physique et de Géologie Dynamique, 3, 5-18.

Bradley V.C., Hutton J.T. and Twidale C.R. 1978. Role of salts in development of granitic tafoni. South Australian Journal of Geology, 86, 647-654.

Cooke, R.U., Varren, A. and Goudie, A. 1993. Desert Geomorphology. London: University College London Press, 526p.

Dana, J.D. 1849. Geology. U.S. Exploring Expedition (1838-1842), V. 10, Philadelphia, C. Herman, 529 p.

Darwin, C.R. 1839. Journal of researches into the natural history and geology of the countries visited during the voyage of HMS Beagle round the world: New York, D. Appleton, 450.

Evans, I.S. 1970. Salt crystallization and rock weathering: A review. Revue de Géomorphologie Dynamique, 19, 153-177.

Folk, R.L., Andrews, P.B. and Lewis, D.W. 1970. Detrital sedimentary rock classification and nomenclature for use in New Zeland. New Zeland Journal of Geology and Geophysics, 13. p. 955.

Gökçen, L.S. 1967. Keşan bölgesinde Eosen-Oligosen sedimantasyonu, Güneybatı Türkiye Trakyası. MTA Bulletin, 69, 1-10.

Kelletat, D. 1980. Studies on the age of honeycombs and tafoni features. Catena, 7, 317-325.

Kellog, H.E. 1973. Geology and Petroleum prospects Gulf of Saros and vicinity southwestern Trace: Ashland Oil of Turkey, Inc. Türkiye Petrol İşleri Genel Müdürlüğü Arşivi, Ankara (unpublished).

McBride, E.F. and Picard, M.D., 2004, Origin of honeycombs and related weathering forms in Oligocene Macigno Sandstone, Tuscan Coasts near Livorno, Italy. Earth Surface Processes and Landforms, 29, 713-735.

Mc Greevy, J.P. 1985. A preliminary scanning electron microscope study of honeycomb weathering of sandstone in a coastal environment. Earth Surface Processes and Landforms, 10, 509-518.

Mellor, A., Short, J. and Kirkby, S.J. 1997. Tafoni in the El Chorro area, Andalucia, southern Spain. Earth Surface Processes and Landforms, 22, 817-833.

Mustoe, G.E. 1982. The origin of honeycomb weathering. Geological Society of America Bulletin, 93, 108-115.

Önem, Y. 1974. Gelibolu ve Çanakkale dolaylarının jeolojisi. TPAO Report No: 877, Ankara (unpublished).

Parkhurst, D.L. and Appello, A.A.J. 1999. User's guide to PHREEQC (version 2) - A computer program for speciation, batch action, one dimensional transport and inverse geochemical modeling: U.S. Geol. Survey, Water-resource Invest., pp. 99-4259.

Rodriguez-Navarro, C., Doehne, E. and Sebastian, E. 1999. Origins of honeycomb weathering: The role of salts and wind. Bull. Geol. Soc. Amer., 111, 1250-1255.

Rondeau, M.A. 1965. Formes d'érosion superficielles dan les grés de Fountainbleau: Association de Géographes Français Bulletin, 334/335, 58-66.

Scherber, R. 1927. Erosionswirkungen an der toskanischen Felsküste. Natur und Museum, 62, 231-234.

Sümengen, M. and Terlemez, İ. 1991. Güneybatı Trakya yöresi Eosen çökellerinin stratigrafisi. MTA Bulletin, 113, 17-30.

Turkington, A.V. and Phillips, J.D. 2004. Cavernous weathering, dynamical instability and self-organization. Earth Surface Processes and Landforms, 29, 665-675.

Turkington, A.V. and Paradise, T.R. 2005. Sandstone weathering: a century of research and innovation. Geomorphology, 67, 229-253

PLATES

PLATE - I

Figure 1- General view of sandstones on which alveolar disintegration develops, in Cape Büyükkemikli. Impure yellow colored, medium to thick bedded, N50E trending sandstone beds. Sandstone conformably overlies the siltstone succession.

Figure 2- Dipping values of southeast dipping (towards the sea) sandstones varies between 38-50. In the NE-SW and NW-SE trending orthogonal and polygonal fractures, resistant shells have been developed due to iron aggragation. These structures are delimit the alveol formation.

Figure 3- Thin section of sandstone with alveolisation. Rock is fine grained quartzarenite. Rock has quartz and plagioclase coming from source rocks of granite and metamorphic rocks, with minor amounts of biotite and muscovite.

Figure 4- Thin section of sandstone without alveolisation. Rock is subgreywacke, and composed of angular grains of quartz with undulose extinction, rock fragments, plagioclase, muscovite and opaque minerals. Rock is clastic, and carbonate cemented.

PLATE - I

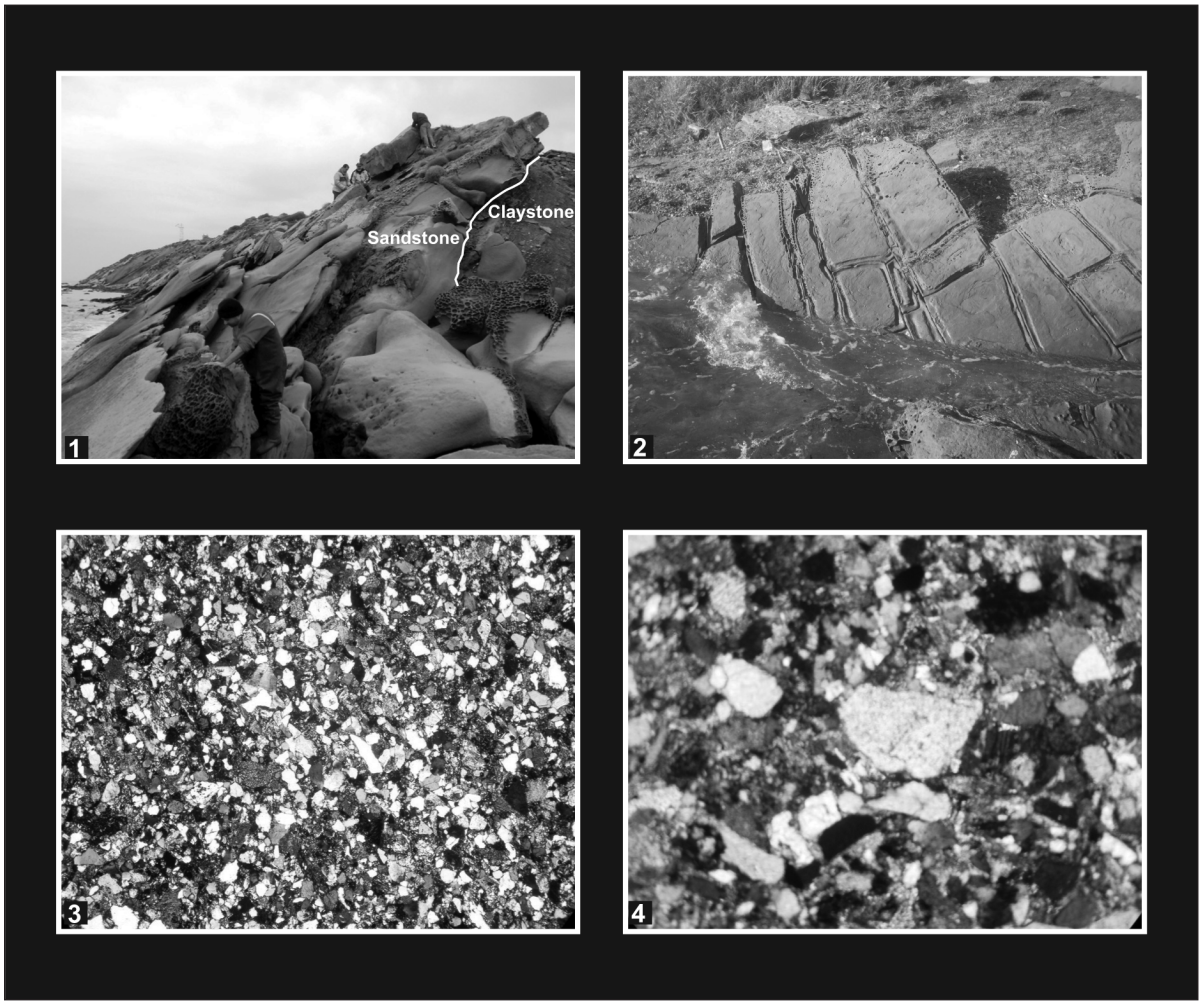

PLATE - II

Figure 1- SEM image of sandstone over which alveolar disintegration developed. Microporosity den sity over rock can be observed. Besides, microporosities with 400 μm-length among ellip soidal microporosities are observed. Fractures were enlarged upto 50 μm as a result of disintegration. Scale: 100 μm.

Figure 2- SEM image of carbonate cemented and muscovite-rich sandstone. Microporosity and microfracture formation on rock was not observed. Scale: 100 μm.

Figure 3- An example for bioerosional impact disturbing morphology of alveolar zones in intratidal zone

Figure 4- The increase of alveol sizes at the second measurement site from intratidal zone. Algae communities cover the heel and walls of alveols. At this part, the crystallization of salt coming from sea water during dry season is effective on disintegration. Arrow in the figure shows the thinning and perforation on the alveol walls.

Figure 5- An example for coalescent alveols located in the intratidal zones.

Figure 6- The impact of organisms at the heel and walls of alveols into the alveolar disintegration. Figure shows that patella and balanus species existing over alveols.

PLATE - II

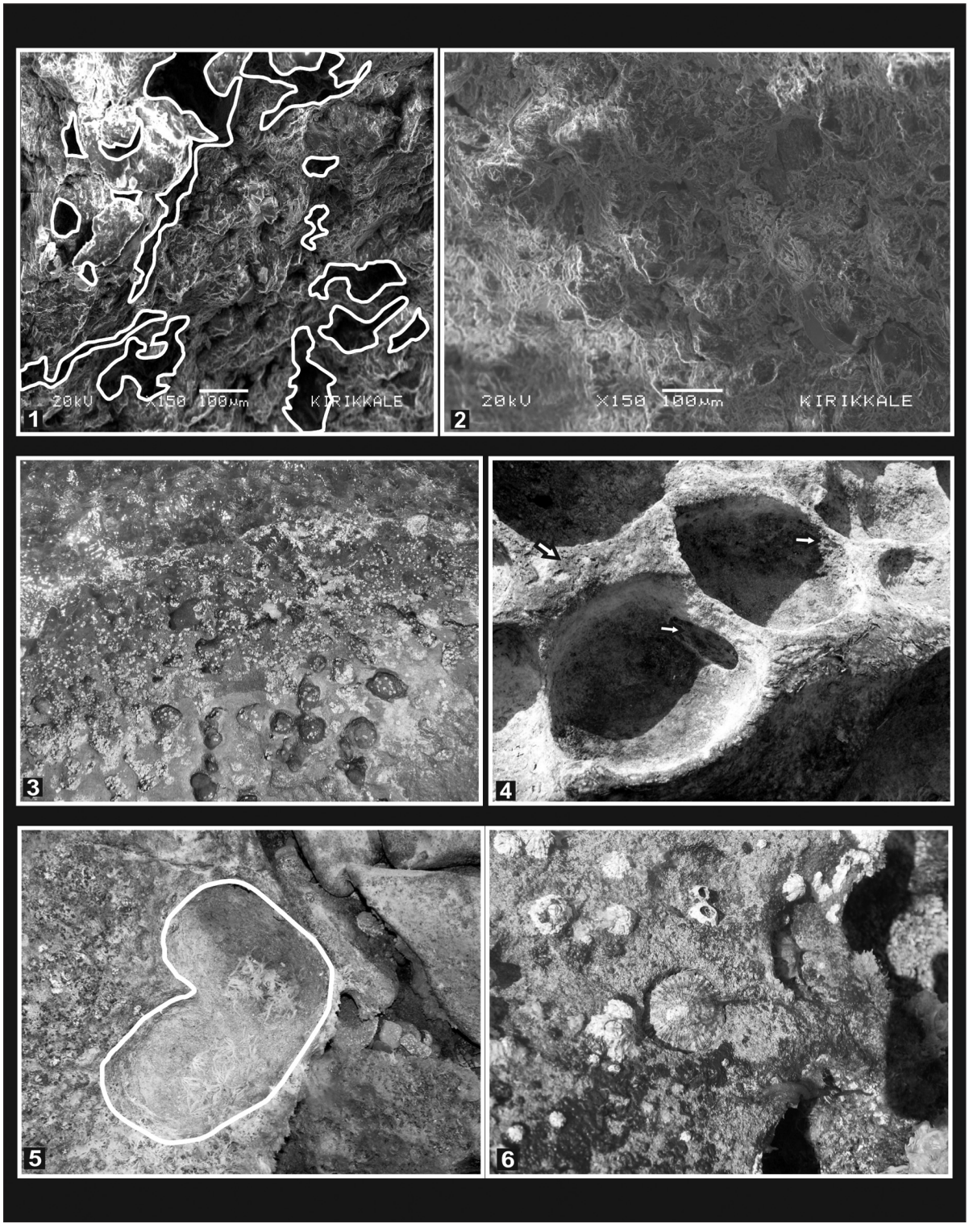
20kV X150 100µm KIRIKKALE
1
20kV X150 100µm KIRIKKALE
2
3
4
5
6

PLATE - III

Figure 1- Alveolar disintegration cells at 1-5 m altitude from sea level. It is observed that alveols join and partially transform into tendrils.

Figure 2- Alveols within the orthogonal pores with iron and calcite infillings. It is observed that alveols are enlarged by joining, and the formation continued over the underlying sandstones. Arrows indicate ellipsoidal Figureli alveols along the fractures.

Figure 3- Initial stage for tafoni formation close to section where Figure 2 was taken. Especially, the evaporation promoting effect of wind over layer surfaces and frontal layers accelerates the crystalization of brine salt and results in tafoni formation.

Figure 4- Rectangular and very brittle alveols (tendril). In such formations, alveol walls are very thin so as different than closed disintegration cells, a few alveol walls have been abandoned.

Figure 5- An example for turtleback examined in study area. Development of such structures is generally related with parts, which are more resistant to disintegration compared to disintegration cells, generally highly weathered and tafoni or cavity-sized.

Figure 6- Alveols with very small sizes compared to lichen communities (*Xantoria* sp.) at the high flat of Cape Büyükkemikli.

PLATE - III

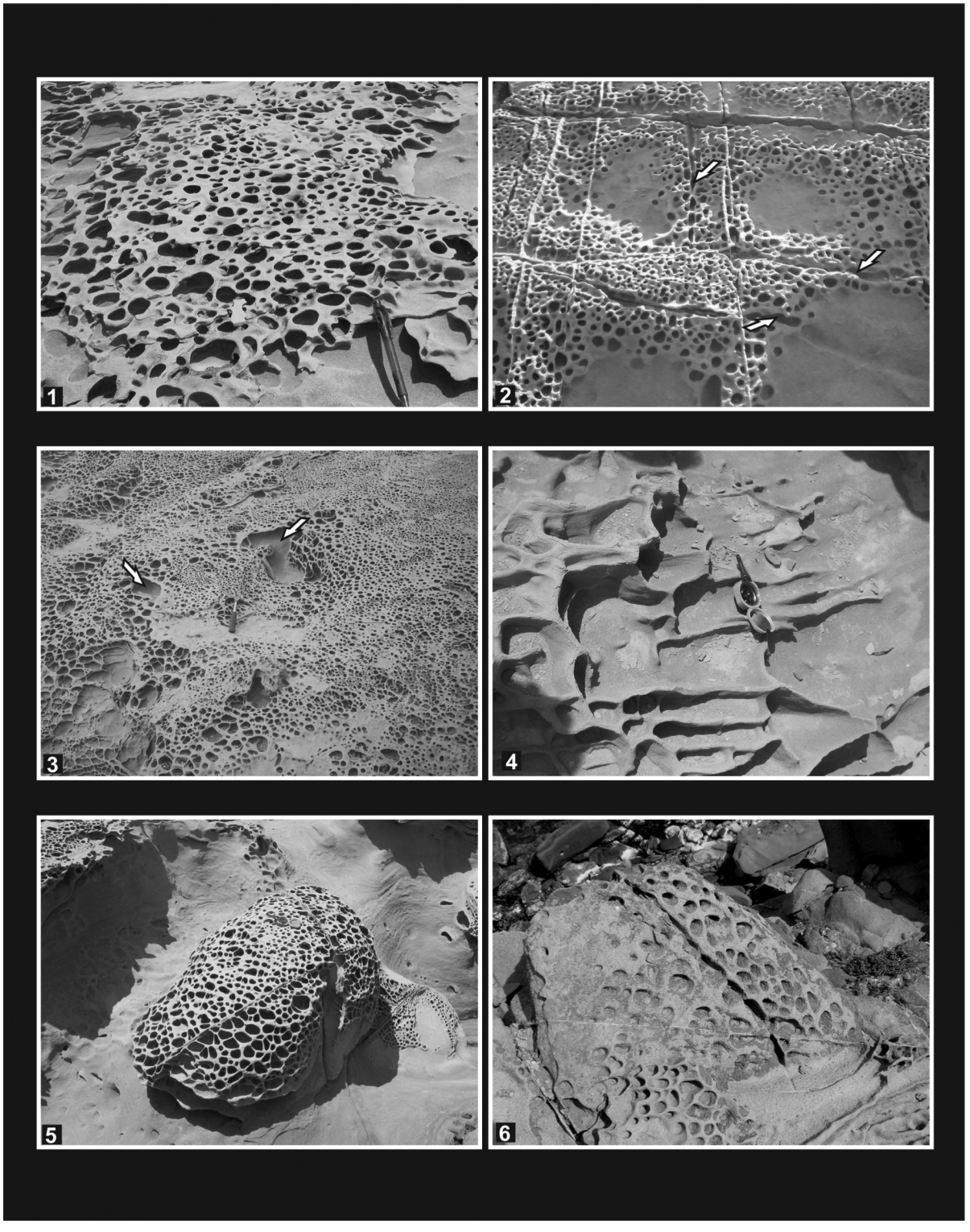

bos sayfa

A NEW AGE RECOVERY ABOUT THE MINING HISTORY IN ANATOLIA; AN ORE HULL OF 2500 YEAR OLD

Ahmet KARTALKANAT*

ABSTRACT.- The radiometric age of an ore hull in 14x28 cm dimensions found in the gallery of an old copper mine in the Çımaklı quarter of Espiye town (Giresun) which was carried out in two different laboratories, has been dated as 2610 ± 70 and 2441 ± 30 yrs. According to these data the age of the material is as old as 2500 yrs, in other word belong to 500' s of BC. However the written sources point that the mining activities started in 183 BC, the ore hull found in the mentioned copper mine shows that the mining activities extend to 500' s of BC in the region. If it is considered that the district of Giresun was under the control of Persian empire between the years of 600-400 BC, the mining activities should belong to this period of time

UNIVERSAL TRANSVERSE MERCATOR AND LAMBERT'S CONFORMAL CONIC PROJECTIONS

Cemal GÖÇMEN **

ABSTRACT.- This article has been prepared with the purposes of giving information about the mapping projections and noticing which points should be taken into account in using these projections. In the article not all of the mapping projections have been described but the two of them, which are mostly used in our works; namely Universal Transverse Mercator and Lambert's Conform Projections which retains the angles have been considered. In the article, for the degree-UTM conversion programs, the importance of the determination of mid-meridian of the zone has been emphasized and the reason of why our maps drawn in Lambert's projections system does not coincide with those drawn in the neighboring countries has been investigated. Further, in the article, the mathematical models used in the map projections have been considered and the interests of human being and works done about the shape and dimensions of the earth in the archaic era has been described under the title of Historical Development.

Key words: Shape of the Earth, UTM Projection, Lambert's Projection.

SHORT NOTE ON POLYPHASES Pd-Pt-Te MINERALISATIONS WHICH IS DETERMINED IN RUTILE BEARING BERIT METAOPHIOLITE CHROMITITES IN KAHRAMANMARAŞ

Hatice KOZLU ERDAL***

ABSTRACT.-The Pt-Pd bearing mineralisations and rutiles are firstly determined in the transition zone (moho-zone) chromitite deposits of the Berit Metaophiolite Massif (BMM) in Kahramanmaraş in our country with this study. The data of electron microprobe analyses of the chromitites indicate that most of the samples are high-Al chromitites with Cr# numbers between (100xCr/(Cr+Al)) 29-37. The rest of the samples are high-Cr chromitites, with Cr# numbers between 60-70. Microscopic examination and electron microprobe analyses of the PPGE and IPGE- enriched samples reveal platinum-group element minerals (PGM) as euhedral (10-15 μm) inclusions in the chromite grains. The PGM hosted by IPGE-rich high-Cr chromitites are primary inclusions of laurite, irarsite, Ir sulphide and erlichmanite. Very small Pd-Pt telluride phases (merenskyite-moncheite) are hosted by polyphase sulphide droplets in the PPGE-rich chromitites of BMM. Considering the different chemical compositions of both chromitite and PGM at Berit, suggested that their parent melts derived from two different magma sources. The presence of hydrosilicate inclusions and the depletion of compatible elements in high-Cr chromitites of BMM suggested that they resulted from higher degrees of partial melting of the upper mantle, probably from second stage melting of a residual source. The Berit chromitites could have formed both from magmas related to the initial rifting process and to subsequent supra-arc magmatism prior to obduction of the host ophiolite. Because of having in different chemical compositions of the Berit chromitites it has been suggested that they could have generated from both of magmas related with the supra-arc magmatism (SSZ) by partial melting process due to metasomatism of oceanic lithosphere (high-Cr chromitites) and subsequently by changing parent magma composition (the high-Al chromitites) in back arc basin environment.

Key words: Kahramanmaraş, Berit, Metaophiolite, Chromitite, Rutile, Pd-Pt-Te